New Insights into Selective Autophagy in Yeast: Studies on Lap3

Takuya Kageyama

DOCTOR OF PHYLOSOPHY

Department of Basic Biology
School of Life Science
The Graduate University for Advanced Studies

2008 (School Year)

DOCTRAL DISSERTATION

New Insights into Selective Autophagy in Yeast: Studies on Lap3

by
Takuya Kageyama

Department of Basic Biology
School of Life Science
The Graduate University for Advanced Studies

March 24, 2009

ACKNOWLEDGEMENTS

March 24, 2009
Takuya Kageyama

National Institute
for Basic Biology

The graduate University
for Advanced Studies

TABLE OF CONTENTS

CHAPTER II
MACHINERY OF THE CVT PATHWAY ACTS FOR DEGRADATION
DURING GLYCEROL GROWTH
IN THE YEAST *Saccharomyces cerevisiae*

ABSTRACT

Cellular activities require the maintenance of balance between the synthesis and degradation of proteins. Regulation of protein degradation is less understood compared to protein synthesis. The ubiquitin-proteasome system contributes to the selective degradation of short-lived protein. Since most of cellular proteins have long lifetimes, the turnover of long-lived proteins is important to the understanding of cell physiology. Macroautophagy (hereafter simply referred to as autophagy) is an intracellular non-selective degradation system, which is well conserved in eukaryotes; autophagy transports cytoplasmic constituents to the lysosomes/vacuoles for degradation. The autophagic degradation is a cellular response to starvation and plays a role in recycling of cytoplasmic components, which is important for cellular remodeling, development, and differentiation. Screens in the yeast *Saccharomyces cerevisiae* have led to the identification of 31 a<u>u</u>topha<u>g</u>y-related (*ATG*) genes involved in autophagy. Much progress has been made in the functional analysis of these genes.

Autophagy is initiated by the sequestration of cytoplasmic constituents in a double-membrane structure, termed the autophagosome. Fusion of an autophagosome membrane with the vacuole membrane results in the delivery of an inner vesicle (*i.e.*, autophagic body). Eighteen Atg proteins comprise the core machinery essential for the biogenesis of the autophagosomes. Immuno-electron microscopy has revealed that ribosomes and typical cytosolic marker enzymes are present in the autophagosomes and autophagic bodies at the same densities as in the cytosol, indicating that autophagy executes a non-selective degradation. If degradation of long-lived proteins is exclusively mediated by autophagy, all proteins might be expected to have similar lifetimes. Long-lived proteins, however, have a variety of lifetimes; therefore, the autophagic process would have some selectivity.

Recently, different molecules or complexes are selectively recognized and delivered to the vacuoles via autophagy. Onodera and Ohsumi have reported (Onodera and Ohsumi, 2005) that Ald6 is preferentially sequestered in autophagosomes and is eliminated from cytoplasm during prolonged starvation; this mechanism, however, is not understood well. Mechanisms of such cargo selection have been well studied for aminopeptidase I (Ape1/Lap4), a vacuole-resident enzyme. Ape1 self-assembles and then forms an aggregate-like structure. Ape1 then is selectively incorporated into autophagosomes and is transported into the vacuole during nitrogen starvation; this process is, however, not degradation but biosynthesis. Little is known about protein that is

selectively degraded by yeast autophagy.

To address the issue of selective degradation via autophagy, I focused on leucine aminopeptidase III (Lap3). *LAP3* was originally isolated, along with *LAP1*/*APE2* and *LAP4*/*APE1*, in a genetic screen and is a widely conserved cytoplasmic cysteine protease among eukaryotes. Lap3 self-assembles in the cytosol, and Lap3 forms homohexameric complex. The first part of this study shows that Lap3 is a selective target of autophagy. When Lap3 tagged with GFP is overexpressed, it forms large aggregates next to the vacuole. Lap3 is transported to the vacuole in a manner dependent on autophagy during nitrogen starvation. Under these conditions, the rate of Lap3 transport is much higher than that of general cytosolic proteins; 27% of Pho8Δ60, an indicator of general cytosolic proteins, is transported to the vacuole within 6 h (Scot et al., 1996), whereas approximately 50% of the Lap3 is transported to the vacuole in 1.5 h. These results show that Lap3 is selectively transported to the vacuole. I also identified that *ATG11* is involved in Lap3 transport. *ATG11* is essential for selective types of autophagy: selective degradation of peroxisomes (pexophagy) and mitochondria (mitophagy).

The amount of Lap3 in the vacuole is apparently reduced after nitrogen-starvation at 3 h. I hypothesized that the reduction in Lap3 was a result of degradation in the vacuole. To examine this possibility, the kinetics of Lap3 degradation via autophagic process was measured using temperature-sensitive (*atg1*^{ts}) cell, which shows that most Lap3 is degraded in the vacuole within a couple of hours. Taken together, Lap3 is a novel target of selective degradation mediated by autophagy during nitrogen starvation. These results are described in *Chapter I*.

The yeast has a unique system, named the <u>c</u>ytoplasm-to-<u>v</u>acuole-<u>t</u>argeting (Cvt) pathway. This pathway utilizes common molecular machinery with autophagy under nutrient-rich and fermentable conditions, and constitutively delivers two vacuole-resident enzymes, Ape1 and α-mannosidase (Ams1), to the vacuole via a double-membrane structure (*i.e.*, Cvt vesicle). The latter half of this study shows that the Cvt pathway is involved in not only a biosynthetic process but also protein degradation.

The Cvt pathway is enhanced during vegetative growth in a medium containing glycerol as non-fermentable carbon source (YPGly). Under the conditions, the amount of vacuole-resident enzymes is increased; the lytic function in the vacuole may be important during YPGly growth, whereas non-selective autophagy is not detectable. I also found that in vacuolar protease-deficient

($pep4\Delta$) cells, single-membrane vesicles accumulate in the vacuole under the conditions. The intravacuolar vesicles are detected in $ATG7$-dependent manner, and ribosomes and membranes are apparently excluded from these vesicles.

To investigate the content of the vesicle, I isolated vacuoles from $pep4\Delta$ cells with or without $ATG7$ and subjected to proteomic analysis, leading to the identification of Lap3 and Ape1. When Lap3 tagged with GFP is endogenously expressed, it forms aggregates next to the vacuole during YPGly growth. Lap3 co-localizes with Ape1 and is transported into the vacuole. This transport requires Atg11 and Atg19, which are essential for the Cvt pathway. Atg19, which is a cargo receptor for Ape1, is immunoprecipitated with Lap3; Atg19 is likely to function as a receptor for Lap3 transport similar to Ape1 transport. These results show that Lap3 is constitutively transport to the vacuole during vegetative growth and is selectively sequestered in the Cvt-related vesicles.

I assumed that Lap3 would be unstable in the vacuole, since Lap3 is the target of selective autophagy (*described in Chapter I*). To test this assumption, the stability of Lap3 in the vacuole was examined in $atg1^{\text{ts}}$ cells. The amount of Lap3 in the vacuole decreased to 50% of its initial level within 1.5 h. I also isolated vacuoles from wild-type and $pep4\Delta$ cells, respectively and subjected to immunoblot, resulting that Lap3 is not detected in wild-type. This result indicates that Lap3 is degraded in the vacuole. Thus, I conclude that machinery of the Cvt pathway can function to eliminate certain proteins during vegetative growth. These results were described in *Chapter II*.

In this study, I revealed the following facts; 1) Lap3 is a novel cargo of selective autophagy during nitrogen starvation, and 2) the Cvt pathway is involved in protein degradation under growth conditions. Recently, protein degradation via autophagic process in mammalian cells was reported to play a crucial role in elimination of aberrant protein complexes, and the process would be performed constitutively and selectively. For instance, polyubiquitinated aggregates are recognized by p62, selectively sequestered by autophagosomes and are degraded in lysosomes. In contrast to p62, we do not know yet whether Lap3 are harmful or disadvantageous for yeast cells. As Lap3 is conserved widely in eukaryotes, it may serve as a model protein for analysis of selective autophagy in other organisms as well. Autophagy has traditionally been described as a non-selective degradation process. Several results shown in this thesis is the first study reporting that autophagy can be involved in selective and/or constitutive protein degradation in yeast cells. This thesis will allow researchers in this field to make new discoveries regarding the regulation and mechanisms of selective and constitutive autophagy.

LIST OF FIGURES AND TABLE

ABBREVIATIONS

A_{600}	absorbance at 600 nm
Ape1	aminopeptidase I
Ams1	α-mannosidase I
CPY	carboxypeptidase
Cvt	cytoplasm to vacuole targeting
DIC	differential interference contrast
DNA	deoxyribonucleic acid
DTT	ditiothreitol
EDTA	ethyleediamine tetra-acetic acid
GFP	green fluorescent protein
KLH	keyhole limpet homocyanin
Lap	leucine aminopeptidase
MALDI-TOF	matrix associated laser deionization-time of flight
mRFP	monomeric red fluorescence
ORF	open reading frame
PAGE	polyacrylamide gel electrophoresis
PAS	pre-autophagosomal structure
PCR	polymerase chain reaction
PrA	proteinase A
PrB	proteinase B
PrC	proteinase C (*i.e.*, CPY)
PGK	phosphoglycerate kinase
SD	synthetic dextrose
SDS	sodium dodecyl sulfate
TBS	tris-buffered saline

INTRODUCTIONS

1. *The Many Routes to the Vacuole -Correlation between vacuole and autophagy-*

    Already more than a half-century has passed since the lytic organelle, named lysosome, was discovered by de Duve using cell fractionation procedures (De Duve and Hooft, 1968). A vacuole in yeast continues to be a very informative model for mammalian lysosome. Multiple pathways can direct proteins to the vacuole in yeast (Figure 1). The "CPY pathway" is the best-studied pathway for newly synthesized vacuolar proteins and involves vesicular transport from the late Golgi through the multivesicular body (MVB) to the vacuole. A number of membrane proteins, including dipeptidyl aminopeptidase B (DPAP-B) and the V-ATPase also transit this pathway (Piper et al., 1995). Carboxypeptidase S (CPS) uses a variation in which it is transported to the MVB as a membrane protein, then inserted into intralumenal vesicles before transport to the vacuole and final processing to remove its membrane domain. The "ALP pathway", named for its alkaline phosphatase cargo, is characterized by direct vesicular transport from the Golgi apparatus to the vacuole (Cowles et al., 1997; Piper et al., 1997; Stepp et al., 1997). In addition, aminopeptidase I (Ape1/Lap4) and α-mannosidase (Ams1) follows an unusual pathway to the vacuole, the Cvt pathway (*see below*), which is characterized by direct transport from the cytosol to the vacuole. In addition to these biosynthetic pathways, multiple proteins are delivered to the vacuole for degradation. Extracellular or cell surface proteins may enter the cells by endocytosis, first transiting to early endosomes and then intersecting the CPY pathway in MVBs before transport to the vacuole (Piper et al., 1995). Intracellular proteins are transported directly to the vacuole and digested in the vacuole under certain conditions. These proteins are generally targeted via the autophagy process (*see below*). In mammalian cells, since then many electron micrographs showing autophagy have been reported in lysosomes from different organs and cultured cells, it is now generally accepted that autophagy is ubiquitous intracellular activity of eukaryotic cells.

2. *Degradation of Short-lived and Long-lived Proteins*

    Proper balance between protein synthesis and degradation (*i.e.*, turnover) is required for cellular homeostasis. Almost proteins have its own lifetime of wide range, from a few minutes to more than ten days (Goldberg and Dice, 1974; Schimke and Doyle, 1970). We do not know yet the determinants of the lifetime of each protein and the exact meaning of protein turnover, but dynamic state of equilibrium itself must be crucial for maintenance of life. Recently, it was realized that proteins are not degraded spontaneously but are degraded rather by active processes.

    These are two major systems of intracellular protein degradation. One is that the

ubiquitin-proteasome system in the cytosol, which is involved in degradation of short-lived, damaged, and/or misfolded proteins (Hershko and Ciechanover, 1998; Hochstrasser, 1991). Target protein to be degraded is a tagged with a ubiquitin and then digested by a huge proteinase complex, proteasome. Both ubiquitination and cleavage processes require ATP hydrolysis, and undergoes with strict recognition of target proteins by the sophisticated ubiquitin ligase system and proteasome. Short-lived proteins play crucial roles in important cellular events as transcriptional regulation and cell cycle model.

Long-lived proteins are believed to be degraded in a specific lytic compartment, lysosomes/vacuoles. So far, several transport routes to the compartment are proposed. General process of degradation of intracellular components in lysosomes/vacuoles is called "Autophagy" in contrast to heterophagy of extracellular materials (Mortimore and Poso, 1987). Macroautophagy is a principal pathway in autophagy, and initiates by enwrapping a portion of cytoplasm by membrane sac called isolation membrane, to form a double membrane structure, named autophagosome (Seglen and Bohley, 1992). Autophagosome then fuses with lysosomes and turns to be autolysosome and its inner membrane and contents are digested for reuse. Microautophagy is a process in which the lysosomes/vacuoles directly engulfs a portion of cytoplasm. Hereafter in this thesis, macroautophagy will be referred simply as autophagy.

Autophagy is characterized as non-selective and bulk degradation of intracellular proteins. More than 90% of intracellular proteins are long-lived proteins, thus turnover of long-lived proteins is important to understand the control of cell growth, because their degradation mainly contributes to the pools of amino acid. Bulk protein degradation is also play roles in the process of starvation response, remodeling, development, differentiation, and, some aspects of organelle homeostasis (Doelling et al., 2002; Levine and Klionsky, 2004; Tsukada and Ohsumi, 1993).

3.   *The Conceptual Model of (Macro)autophagy*

These years, genetically and molecular biological approaches using the yeast *Saccharomyces cerevisiae* have begun to unravel a molecular dynamics of autophagy. The general mechanism of autophagy is the sequestration of cytoplasmic cargoes that have to be degraded into large double-membrane vesicle (*i.e.*, autophagosome), which then fuse with the lysosomes/vacuoles liberating the internal vesicles, also called an autophagic body, into the interior of this organelle where, together with the cargo, it is degraded by vacuolar hydrolases (Figure 2). The biogenesis and consumption of autophagosome can be divided into four discrete morphological steps: (i) induction and expansion that is marked by the initiation of sequestration; (ii) completion during which the cargo becomes enclosed within a completed vesicle; (iii) docking and fusion where the

outer vesicle membrane tethers to and fuses with the lysosomes/vacuoles; and (iv) breakdown that involves lysis of the inner vesicle and degradation of the cargo (Suzuki and Ohsumi, 2007). Autophagosome is formed from small initial cisternae also termed isolation membrane. It remains unknown from which organelle and how this compartment is generated. Studies in mammalian cells have indicated that several of these isolation membranes are present in the cytoplasm in resting situations. After autophagy induction, they simultaneously give rise to numerous autophagosome (Mizushima, 2005; Suzuki and Ohsumi, 2007).

The autophagic process in yeast such as *Saccharomyces cerevisiae* and *Pichia pastoris*, however, is different from the one in mammals in two aspects. First, it seems that the isolation membrane does not find (Reggiori et al., 2005). Second, autophagosome is formed at a single perivacuolar location one after the other (Suzuki and Ohsumi, 2007). This specialized site has been defined as the pre-autophagosomal structure (PAS). The PAS is believed to be an independent structure where the double-membrane vesicle formation occurs after the induction of the sequential recruitment of the proteins required for this process. Because of this dynamic aspect, the PAS cannot be considered as the isolation membrane but should be seen as a series of autophagosomal intermediates in perpetual transformation and progression to become an autophagosome.

4. *The ATG Genes and the Core Autophagy Machinery*

Genetic screens in *S. cerevisiae* have led to the identification of 31 genes essential for autophagy that are termed *ATG*, as well as the steps of the autophagosome formation in which they act (Figure 3) (Reggiori, 2006). However, the precise molecular function of most of them remains unclear. Eighteen *ATG*-gene-products (Atg proteins) form the basic machinery essential for the biogenesis of double-membrane vesicles in all eukaryotes (Figure 3). These proteins mediate the induction and expansion and/or completion steps and are required for both selective and nonselective types of autophagy (Figure 2, *steps 1* and *2*). In *S. cerevisiae*, these proteins, most of which are soluble, sequentially associate with the PAS and the temporal order of recruitment has been determined (Figure 4) (Suzuki and Ohsumi, 2007).

The Atg1 protein kinase is one of the first Atg components to be found at the yeast PAS. Several signaling pathways have been shown to regulate the induction of autophagy in response to various stimuli (Nair and Klionsky, 2005). The main target of these cascades is Atg1, and its activity is regulated by phosphorylation and dephosphorylation reactions (Nair and Klionsky, 2005). Except for its autophosphorylation, no other substrate of Atg1 has been characterized. Atg1 associates with the Atg13 but also multiple other Atg proteins, such as Atg11 or Atg17 that are

specific for selective or non-selective types of autophagy, respectively (Nair and Klionsky, 2005). The phosphorylation status of Atg1 seems to lead to conformational changes that modulate its association with its interacting partners. In higher eukaryotes, changes in Atg1 levels alter the activity of autophagy (Scott et al., 2007). Taken together, Atg1 is believed to be the key autophagy regulator.

Induction of autophagy triggers the simultaneous expansion and nucleation of the isolation membrane (Figure 2, *step 1*). Two ubiquitin-like molecules, Atg5 and Atg8, have a key role in this step, which also involves the acquisition of additional membranes. In yeast, Atg5 requires the autophagy-specific-PI3K (hereafter refer to AS-PI3K) and Atg1 to be recruited to the PAS, whereas in mammalian cells, Atg5 appears to associate constitutively to the isolation membrane through a process that also involves PtdIns3P (Mizushima et al., 2001; Suzuki et al., 2007). Atg5 can be covalently conjugated to Atg12, and this linkage is mediated by a system similar to that used for ubiquitination, where Atg7 acts as an E1-activating enzyme and Atg10 as an E2 ligase (Levine and Klionsky, 2004; Reggiori, 2006). In mammalian cells, induction of autophagy leads to the conjugation of Atg12 to Atg5 and that event seems to trigger the expansion of the isolation membrane (Figure 2, *step 1*), which also involves the association of Atg16 to the Atg5–Atg12 conjugate (Mizushima et al., 2001). Because the Atg16-Atg5–Atg12 complex oligomerizes and localizes along the external surface of the forming autophagosomes, it has been proposed that it could act as a potential coat mediating the nucleation of the growing isolation membrane (Mizushima et al., 1999). Atg8 is targeted to membranes through the unconventional linkage to the lipid phosphatidylethanolamine (PE). After synthesis, the C-terminal amino acid of Atg8 is clipped by the Atg4 protease, exposing a glycine residue and a second ubiquitination-like system, where Atg7 acts as an E1-activating enzyme and Atg3 as an E2 ligase, leads to its lipidation (Ichimura et al., 2000). Activation of the Atg5 conjugation system by autophagy induction triggers the Atg8 conjugation system that directs the association of Atg8 to the PAS (Suzuki et al., 2007). This feature and the fact that in yeast, *ATG8* deletion leads to very small autophagosomes (Nakatogawa et al., 2008), shows a possible role of this ubiquitin-like protein in the recruitment of membranes to the PAS. This hypothesis is supported by the recent finding that Atg8 acquires fusogenic properties by a conformational change induced by its linkage to PE (Ohsumi, 2001). This property could be used for the fusion of membranous structures into autophagosomes (Ohsumi, 2001; Suzuki et al., 2007).

Once autophagosome are complete, all the Atg proteins peripherally associated to the surface of these vesicles are released into the cytoplasm (Ohsumi, 2001). This includes the dissociation of the Atg8 pool bound to the external side of autophagosomes by the Atg8-processing enzyme Atg4, which cleaves the lipid anchor (Suzuki et al., 2007). This uncoating event seems to be a

prerequisite for the following fusion between autophagosomes and lysosomes/vacuoles. Another event occurring at this stage is the retrieval of Atg9. The Atg2-Atg18 complex is responsible for the Atg9 retrieval from the PAS and/or complete autophagosome, and the recruitment of this complex to the PAS requires Atg1 and AS-PI3K (Suzuki et al., 2007).

Once uncoated, autophagosome dock and fuse with the lysosomes (Figure 2). These two events are catalyzed by a set of proteins also used by other pathways that require the docking to and the fusion with the lysosomes/vacuoles (Reggiori, 2006). This convergence between transport routes is reflected at the step of the autophagic body breakdown as well, where the degradation of subvacuolar vesicles is mediated by common proteases (Reggiori, 2006).

5. *Selective Types of Autophagy*

Several selective types of autophagy have been described, and in numerous cases a specific name has been assigned to them (Figure 6). In addition to the basic Atg machinery, these processes use additional Atg proteins that are required to either guarantee their specificity or mediate membrane traffic (Figure 6).

5-1 *The Cvt Pathway*

The best-characterized selective type of autophagic process is the Cvt pathway, and its study has provided a possible model for how specific cargoes are enwrapped by autophagosomes (*see below*). The Cvt pathway is a selective transport for Ape1/Lap4 and Ams1, and occurs constitutively in yeast, *Saccharomyces cerevisiae*. The classical model for deriver of hydrolases to the vacuole is via a portion of the secretory pathway. Proteins transit from the endoplasmic reticulum (ER) thought the Golgi complex and are sorted away from other proteins in the secretory pathway, diver to the endosome, and then to the vacuole. Analysis of Ape1/Lap4 and Ams1, which are vacuole soluble hydrolases, indicate that they are not transported via secretory pathway (Klionsky et al., 1992; Yoshihisa and Anraku, 1990; Yoshihisa et al., 1988). It is constitutively synthesized as an inactive precursor form (61 kDa) in the cytosol. It is targeted to the vacuole, and then processed by vacuolar proteinase B (Prb1) at its unusual 45-amino-acid-long-N-terminal region to become mature (55 kDa) (Segui-Real et al., 1995).

After synthesis, precursor Ape1 (prApe1) rapidly is self-oligomerized in the cytosol into the dodecamer (Figure 4; Figure 5) (Kim et al., 1997). Then the complex (Cvt complex) is specifically enwrapped by the Cvt vesicles and is delivered directly from cytoplasm to the vacuole; therefore, this pathway utilizes a subset of the autophagy machinery (Harding et al., 1996) (Figure 5). The morphological studies of the Cvt pathway using an electron microscopy showed that the Cvt

complex is enclosed by autophagosome-like membrane and the Cvt bodies inside the vacuole was detected in vacuolar hydrolase deficient cells (Figure 5). The membrane topology between autophagosome and the Cvt vesicles quite similar, although they are made in different sizes. The size of autophagosome is 300-900 nm, whereas that of the Cvt vesicle is 140-160 nm (Baba et al., 1997; Takeshige et al., 1992). Under starvation conditions, since the Cvt complex is enriched in the autophagosome, autophagy carried out the transport of precursor Ape1.

5-2 *Mitophagy*

Mitochondria are the power stations of the cell, and they generate most of the ATP required to keep the majority of the cellular functions operational. During this process, harmful reactive oxygen species (ROS) are generated. Over time, ROS production increases because aged and/or damaged mitochondria produce and release more ROS, thereby increasing the amount of cellular alterations. In order to maintain healthy cells, defective mitochondria must, therefore, be eliminated. A link between ROS and the induction of autophagy has recently been revealed (Kim et al., 2007). Nutrient starvation stimulates the production of ROS that is essential for the induction of autophagy. Indeed, treatment with antioxidants impairs autophagosome formation. This discovery suggests the possible scenario that damaged mitochondria activate mitophagy by uncontrolled release of ROS. How mitochondria are selectively sequestered into autophagosome has ever been unknown. Recently, studies in *S. cerevisiae* have shown that *ATG11*, in which it appears to be a common adaptor protein for specific types of autophagy, is essential for the process (Figure 3; Figure 6) (Kanki and Klionsky, 2008), suggesting that mitophagy is a specific process.

5-3 *Pexophagy*

The abundance of peroxisomes can rapidly change in response to changing environmental and/or physiological conditions. For example, the number of peroxisomes rapidly increases upon induction of peroxisome proliferation. In rodents, this is observed upon administration of peroxisomes proliferators, whereas in yeast species, peroxisome proliferation is induced during growth of cells on specific carbon sources (*e.g.*, oleic acid or methanol). Generally, these responses are the result of metabolic adaptations to new physiological conditions that require peroxisomal metabolism. The opposite process, a rapid decrease in peroxisome abundance, can also be induced. Thus, when the peroxisome proliferation stimulus is removed, and/or peroxisomal metabolism is not required anymore, peroxisomes are degraded by lysosomes/vacuoles through autophagic pathways. This process is called "pexophagy", and occurs selectively towards peroxisomes. Therefore, it is distinct from non-selective autophagy, which is

generally induced by nutrient starvation.

The abundance of peroxisomes within a cell can rapidly decrease by selective autophagic degradation (also designated pexophagy). Studies in yeast species have shown that at least two modes of peroxisome degradation are employed, namely macropexophagy and micropexophagy (Sakai et al., 2006). During macropexophagy, peroxisomes are individually sequestered by membranes, thus forming a pexophagosome. This structure fuses with the vacuolar membrane, resulting in exposure of the incorporated peroxisome to vacuolar hydrolases. During micropexophagy, a cluster of peroxisomes is enclosed by vacuolar membrane protrusions and/or segmented vacuoles as well as a newly formed membrane structure, the micropexophagy-specific membrane apparatus (MIPA), which mediates the enclosement of the vacuolar membrane. Subsequently, the engulfed peroxisome cluster is degraded.

5-4 *ER-phagy*

One of the main functions of the ER is the folding and processing of newly synthesized proteins destined for the plasma membrane, the extracellular space and almost all subcellular organelles including the ER itself. These events are co-ordinated by a highly regulated process of quality control performed by a plethora of chaperones, enzymes and other factors present in the ER lumen. In certain stress conditions, the balance between the folding capacity of the ER and the number of nascent proteins is shifted in such a way that there is an excess of unfolded proteins. An ER-to-nucleus signaling pathway, the unfolded protein response (UPR), senses this accumulation (Bernales et al., 2007). The UPR also modulates the expansion of the ER volume by increasing the size of its limiting membrane and that accommodates the folding of a large number of proteins(Bernales et al., 2007). When the UPR system is no longer necessary and becomes inactivated, the ER re-establishes its homeostatic volume. Recently, autophagy participates in the elimination of the superfluous ER (Bernales et al., 2007). *atg1Δ*, *atg8Δ*, *atg9Δ*, and *atg16Δ* cells lead to a growth defect upon UPR induction (Bernales et al., 2007). ER-Phagy also required additional genes when compared with the non-selective autophagy, including *ATG19* and *ATG20*, two genes also involved in two other selective types of yeast autophagy (Figure 3; Figure 6), suggesting that ER-phagy is a specific process.

5-5 *Ribophagy*

Starved cells induce autophagy, by which ribosomes are non-selectively delivered to and are degraded in the vacuole, together with other cytoplasmic constituents. In addition, ribosomes are selectively incorporated into autophagosomes. Recently, Ubp3/Bre5 is specifically involved in the uptake of ribosomal 60S subunits into autophagosome (Kraft et al., 2008). Several GFP-fused

ribosomal proteins of both 60S and 40S subunits, which were functional and correctly assembled into ribosomes, is delivered to and degraded in the vacuole of nitrogen-starved cells in an autophagy-dependent manner. This is not surprising, given that autophagy randomly delivers cytoplasmic constituents to the vacuole. However, when autophagic degradation of ribosomal proteins is compared with that of other cytoplasmic proteins, ribosomal degradation has occurred more extensively. This suggests that ribosomes are preferentially targeted to the autophagic pathway under conditions of nitrogen starvation. Ubp3/Bre5 is also specifically involved in the uptake of ribosomal 60S subunits into autophagosomes; however, it is not clear how Ubp3/Bre5 mediate selective autophagic degradation of ribosomal 60S subunits.

5-6   *Targeting of protein aggregation*

Several lines of evidence have indicated that the elimination of the toxic aggregates by autophagy is a selective process (*i.e.*, aggrephagy) (Figure 6). For instance, the study of p62/sequestosome 1 (SQSTM1) has provided a possible model for how protein aggregates are recognized and selectively eliminated by autophagosomes. The p62/SQSTM1 interacts directly with Atg8 (Pankiv et al., 2007). In the absence of p62/SQSTM1, protein aggregates are not enwrapped by autophagosomes, strongly suggesting that p62/SQSTM1 mediates the recognition of polyubiquitinated proteins by double-membrane vesicles (Pankiv et al., 2007). It also became clear that autophagy not only has a role in eliminating aberrant protein complexes in pathological conditions but also its cellular basal activity prevents the formation of aggregates that could cause cell death in neurons (Rubinsztein, 2006). The specific knockout of either *ATG5* or *ATG7* in murine neurons leads to a time-dependent formation of ubiquitinated protein aggregates that resemble those observed in neurodegenerative disorders. These mice do not express any disease-associated mutant proteins and thus are not particularly prone to form aggregates. This crucial finding demonstrates that autophagy is also of vital importance in sustaining healthy aggregate-free neuronal cells.

6.   *The Aim of This Study*

Much progress has been made in the functional analysis of Atg proteins. Atg proteins also function in the steps of autophagosome formation. One of the interesting subjects remained is an issue what is the substrate selectively in autophagy. Ohsumi and co-workers previously revealed that autophagy transports cytoplasmic constituents to the vacuole non-selectively in morphological and biochemical experiments. Immuno-electoron microscopy has shown that cytosolic ribosomes and typical cytosolic marker enzymes, such as alcohol dehydrogenase (Adh1)

and phosphoglycerate kinase (Pgk1), are present in the autophagosomes and autophagic bodies at the same densities as in the cytosol (Figure 7) (Baba et al., 1994). The measurement of the enzymatic activities of Adh1, Pgk1, glcose-6-phosphate dehydrogenase (G6pdh), and glutamate dehydrogenase also supports this conclusion (T. Noda and Y. Ohsumi., unpublished data) (Takeshige et al., 1992).

If degradation of long-lived proteins is exclusively mediated by autophagy, all proteins might be expected to have similar lifetimes. Long-lived proteins, however, have a variety of lifetimes; thus, the autophagic process might have some selectivity. It is known that Ape1 and Ams1 (via the Cvt pathway) (Figure 5; Figure 6), fructose-1,6-bisphosphatase (Fbp1) via the vacuolar import and degradation pathway; *i.e.*, the Vid pathway (Brown et al., 2008; Chiang and Chiang, 1998; Hoffman and Chiang, 1996) are selectively transported from the cytoplasm to the vacuole. Previously, Onodera and Ohsumi showed that Ald6, alcohol dehydrogenase, is preferentially sequestered in autophagosome (Onodera and Ohsumi, 2005). Chiba *et al*. observed that autophagosome-like structure selectively sequestered to the part of chloroplasts to the exclusion of thylakoid membranes termed Rubisco containing bodies in wheat leaf cells during natural senescence (Chiba et al., 2003) . Microautophagy may have the substrate selectivity potentially, in fact, peroxisomes and cell nucleus are imported to the vacuole via the process via microautophagy (Sakai et al., 1998; Tuttle and Dunn, 1995), and via piecemeal macroautophagy (Roberts et al., 2003). To investigate the possibility of selective autophagic degradation, I focused on Lap3 in this study. GFP-fused Lap3 forms an aggregate associating with the Cvt complex and then selectively transported to the vacuole together with Ape1. Lap3 is degraded in the vacuole, whereas Ape1 is relatively stable. I propose that Lap3 is a novel target of selective degradation mediated by the machinery of the Cvt pathway and autophagy.

7. *References*

Baba, M., M. Osumi, S.V. Scott, D.J. Klionsky, and Y. Ohsumi. 1997. Two distinct pathways for targeting proteins from the cytoplasm to the vacuole/lysosome. *J. Cell Biol.*   139:1687-95.

Baba, M., K. Takeshige, N. Baba, and Y. Ohsumi. 1994. Ultrastructural analysis of the autophagic process in yeast: detection of autophagosomes and their characterization. *J. Cell Biol.* 124:903-13.

Bernales, S., S. Schuck, and P. Walter. 2007. ER-phagy: selective autophagy of the endoplasmic reticulum. *Autophagy*. 3:285-7.

Brown, C.R., A.B. Wolfe, D. Cui, and H.L. Chiang. 2008. The vacuolar import and degradation pathway merges with the endocytic pathway to deliver fructose-1,6-bisphosphatase to the vacuole for degradation. *J. Biol. Chem*. 283:26116-27.

Chiang, M.C., and H.L. Chiang. 1998. Vid24p, a novel protein localized to the fructose-1,6-bisphosphatase-containing vesicles, regulates targeting of fructose-1,6-bisphosphatase from the vesicles to the vacuole for degradation. *J. Cell Biol.* 140:1347-56.

Chiba, A., H. Ishida, N.K. Nishizawa, A. Makino, and T. Mae. 2003. Exclusion of ribulose-1,5-bisphosphate carboxylase/oxygenase from chloroplasts by specific bodies in naturally senescing leaves of wheat. *Plant Cell Physiol.* 44:914-21.

Cowles, C.R., G. Odorizzi, G.S. Payne, and S.D. Emr. 1997. The AP-3 adaptor complex is essential for cargo-selective transport to the yeast vacuole. *Cell.* 91:109-18.

De Duve, C., and C. Hooft. 1968. [Quinquennial prizes of the medical sciences, period 1961-1965. Address by Prof. Chr. De Duve]. *Verh K Vlaam Acad Geneeskd Belg.* 30:381-8.

Doelling, J.H., J.M. Walker, E.M. Friedman, A.R. Thompson, and R.D. Vierstra. 2002. The *APG8/12*-activating enzyme *APG7* is required for proper nutrient recycling and senescence in Arabidopsis thaliana. *J. Biol. Chem.* 277:33105-14.

Goldberg, A.L., and J.F. Dice. 1974. Intracellular protein degradation in mammalian and bacterial cells. *Annu. Rev. Biochem.* 43:835-69.

Harding, T.M., A. Hefner-Gravink, M. Thumm, and D.J. Klionsky. 1996. Genetic and phenotypic overlap between autophagy and the cytoplasm to vacuole protein targeting pathway. *J. Biol. Chem.* 271:17621-4.

Hershko, A., and A. Ciechanover. 1998. The ubiquitin system. *Annu. Rev. Biochem.* 67:425-79.

Hochstrasser, M. 1991. Functions of intracellular protein degradation in yeast. *Genet. Eng. (N Y).* 13:307-29.

Hoffman, M., and H.L. Chiang. 1996. Isolation of degradation-deficient mutants defective in the targeting of fructose-1,6-bisphosphatase into the vacuole for degradation in *Saccharomyces cerevisiae*. *Genetics.* 143:1555-66.

Ichimura, Y., T. Kirisako, T. Takao, Y. Satomi, Y. Shimonishi, N. Ishihara, N. Mizushima, I. Tanida, E. Kominami, M. Ohsumi, T. Noda, and Y. Ohsumi. 2000. A ubiquitin-like system mediates protein lipidation. *Nature.* 408:488-92.

Kanki, T., and D.J. Klionsky. 2008. Mitophagy in yeast occurs through a selective mechanism. *J. Biol. Chem.* 283:32386-93.

Kim, I., S. Rodriguez-Enriquez, and J.J. Lemasters. 2007. Selective degradation of mitochondria by mitophagy. *Arch. Biochem. Biophys.* 462:245-53.

Kim, J., S.V. Scott, M.N. Oda, and D.J. Klionsky. 1997. Transport of a large oligomeric protein by the cytoplasm to vacuole protein targeting pathway. *J. Cell Biol.* 137:609-18.

Klionsky, D.J., R. Cueva, and D.S. Yaver. 1992. Aminopeptidase I of *Saccharomyces cerevisiae* is localized to the vacuole independent of the secretory pathway. *J. Cell Biol.* 119:287-99.

Kraft, C., A. Deplazes, M. Sohrmann, and M. Peter. 2008. Mature ribosomes are selectively degraded upon starvation by an autophagy pathway requiring the Ubp3p/Bre5p ubiquitin protease. *Nat. Cell Biol.* 10:602-10.

Levine, B., and D.J. Klionsky. 2004. Development by self-digestion: molecular mechanisms and biological functions of autophagy. *Dev. Cell*. 6:463-77.

Mizushima, N. 2005. The pleiotropic role of autophagy: from protein metabolism to bactericide. *Cell Death Differ.* 12 Suppl 2:1535-41.

Mizushima, N., T. Noda, and Y. Ohsumi. 1999. Apg16p is required for the function of the Apg12p-Apg5p conjugate in the yeast autophagy pathway. *EMBO J.* 18:3888-96.

Mizushima, N., A. Yamamoto, M. Hatano, Y. Kobayashi, Y. Kabeya, K. Suzuki, T. Tokuhisa, Y. Ohsumi, and T. Yoshimori. 2001. Dissection of autophagosome formation using Apg5-deficient mouse embryonic stem cells. *J. Cell Biol.* 152:657-68.

Mortimore, G.E., and A.R. Poso. 1987. Intracellular protein catabolism and its control during nutrient deprivation and supply. *Annu. Rev. Nutr.* 7:539-64.

Nair, U., and D.J. Klionsky. 2005. Molecular mechanisms and regulation of specific and nonspecific autophagy pathways in yeast. *J. Biol. Chem.* 280:41785-8.

Nakatogawa, H., K. Oh-oka, and Y. Ohsumi. 2008. Lipidation of Atg8: how is substrate specificity determined without a canonical E3 enzyme? *Autophagy*. 4:911-3.

Ohsumi, Y. 2001. Molecular dissection of autophagy: two ubiquitin-like systems. *Nat. Rev. Mol. Cell Biol.* 2:211-6.

Onodera, J., and Y. Ohsumi. 2005. Autophagy is required for maintenance of amino acid levels and protein synthesis under nitrogen starvation. *J. Biol. Chem.* 280:31582-6.

Pankiv, S., T.H. Clausen, T. Lamark, A. Brech, J.A. Bruun, H. Outzen, A. Overvatn, G. Bjorkoy, and T. Johansen. 2007. p62/SQSTM1 binds directly to Atg8/LC3 to facilitate degradation of ubiquitinated protein aggregates by autophagy. *J. Biol. Chem.* 282:24131-45.

Piper, R.C., N.J. Bryant, and T.H. Stevens. 1997. The membrane protein alkaline phosphatase is delivered to the vacuole by a route that is distinct from the *VPS*-dependent pathway. *J. Cell Biol.* 138:531-45.

Piper, R.C., A.A. Cooper, H. Yang, and T.H. Stevens. 1995. *VPS27* controls vacuolar and endocytic traffic through a prevacuolar compartment in *Saccharomyces cerevisiae. J. Cell Biol.* 131:603-17.

Reggiori, F. 2006. 1. Membrane origin for autophagy. *Curr. Top Dev. Biol.* 74:1-30.

Reggiori, F., I. Monastyrska, T. Shintani, and D.J. Klionsky. 2005. The actin cytoskeleton is required for selective types of autophagy, but not nonspecific autophagy, in the yeast *Saccharomyces cerevisiae. Mol. Biol. Cell*. 16:5843-56.

Roberts, P., S. Moshitch-Moshkovitz, E. Kvam, E. O'Toole, M. Winey, and D.S. Goldfarb. 2003. Piecemeal microautophagy of nucleus in *Saccharomyces cerevisiae. Mol. Biol. Cell*. 14:129-41.

Rubinsztein, D.C. 2006. The roles of intracellular protein-degradation pathways in neurodegeneration. *Nature*. 443:780-6.

Sakai, Y., A. Koller, L.K. Rangell, G.A. Keller, and S. Subramani. 1998. Peroxisome degradation by microautophagy in Pichia pastoris: identification of specific steps and morphological intermediates. *J. Cell Biol*. 141:625-36.

Sakai, Y., M. Oku, I.J. van der Klei, and J.A. Kiel. 2006. Pexophagy: autophagic degradation of peroxisomes. *Biochim. Biophys. Acta*. 1763:1767-75.

Schimke, R.T., and D. Doyle. 1970. Control of enzyme levels in animal tissues. *Annu. Rev. Biochem.* 39:929-76.

Scott, R.C., G. Juhasz, and T.P. Neufeld. 2007. Direct induction of autophagy by Atg1 inhibits cell growth and induces apoptotic cell death. *Curr. Biol*. 17:1-11.

Seglen, P.O., and P. Bohley. 1992. Autophagy and other vacuolar protein degradation mechanisms. *Experientia*. 48:158-72.

Segui-Real, B., M. Martinez, and I.V. Sandoval. 1995. Yeast aminopeptidase I is post-translationally sorted from the cytosol to the vacuole by a mechanism mediated by its bipartite N-terminal extension. *EMBO J*. 14:5476-84.

Stepp, J.D., K. Huang, and S.K. Lemmon. 1997. The yeast adaptor protein complex, AP-3, is essential for the efficient delivery of alkaline phosphatase by the alternate pathway to the vacuole. *J. Cell Biol*. 139:1761-74.

Suzuki, K., Y. Kubota, T. Sekito, and Y. Ohsumi. 2007. Hierarchy of Atg proteins in pre-autophagosomal structure organization. *Genes Cells*. 12:209-18.

Suzuki, K., and Y. Ohsumi. 2007. Molecular machinery of autophagosome formation in yeast, *Saccharomyces cerevisiae*. *FEBS Lett*. 581:2156-61.

Takeshige, K., M. Baba, S. Tsuboi, T. Noda, and Y. Ohsumi. 1992. Autophagy in yeast demonstrated with proteinase-deficient mutants and conditions for its induction. *J. Cell Biol*. 119:301-11.

Tsukada, M., and Y. Ohsumi. 1993. Isolation and characterization of autophagy-defective mutants of *Saccharomyces cerevisiae*. *FEBS Lett*. 333:169-74.

Tuttle, D.L., and W.A. Dunn, Jr. 1995. Divergent modes of autophagy in the methylotrophic yeast Pichia pastoris. *J. Cell Sci*. 108 (Pt 1):25-35.

Yoshihisa, T., and Y. Anraku. 1990. A novel pathway of import of alpha-mannosidase, a marker enzyme of vacuolar membrane, in *Saccharomyces cerevisiae*. *J. Biol. Chem*. 265:22418-25.

Yoshihisa, T., Y. Ohsumi, and Y. Anraku. 1988. Solubilization and purification of alpha-mannosidase, a marker enzyme of vacuolar membranes in *Saccharomyces cerevisiae*. *J. Biol. Chem*. 263:5158-63.
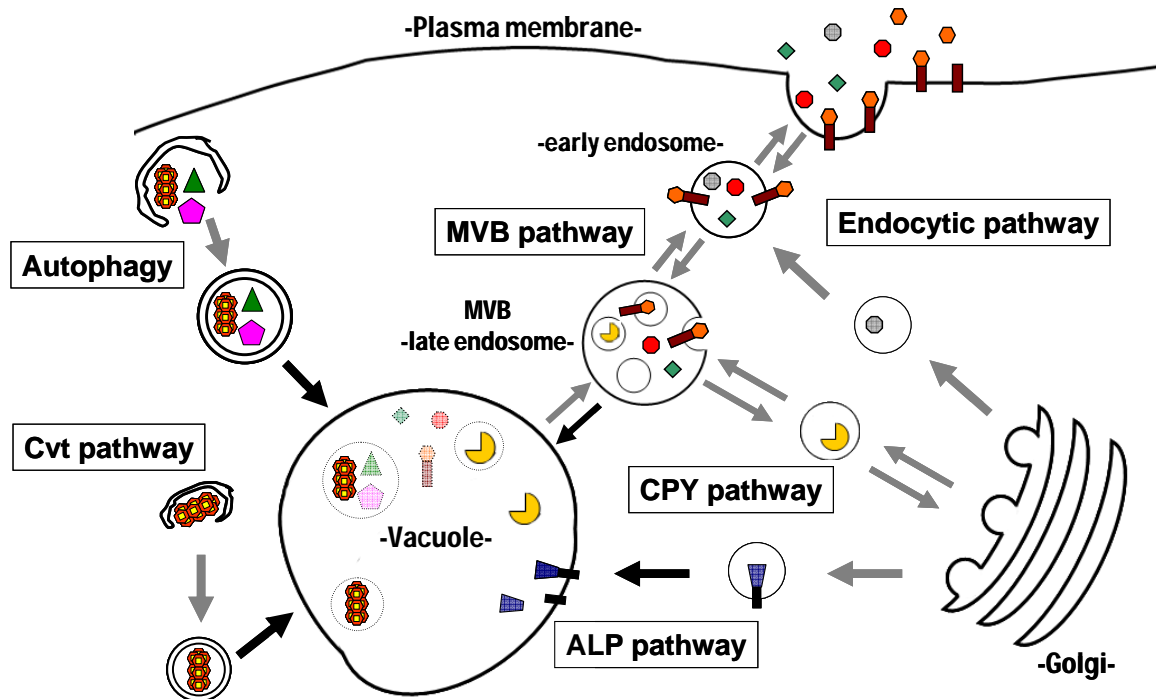
Figure 1. Trafficking pathways to and from the vacuole.

Multiple vesicular pathways deliver proteins to and from the vacuole. Resident vacuolar proteins are sent to the vacuole by several biosynthetic pathways, while proteins targeted for degradation may be sent via endocytosis or autophagy. Biosynthetic pathways: The ALP pathway delivers cargo from the late Golgi to the vacuole. The CPY pathway also starts from the late Golgi, but traverses multivesicular bodies (MVBs) before reaching the vacuole. The Cvt pathway delivers biosynthetic cargo from the cytosol to the vacuole in a process that has common components with autophagy. Trafficking pathways away from the vacuole may recycle membrane and proteins to the endocytic or CPY pathways. Degradative pathways: Endocytosis transports both soluble and membrane-bound cargo from the plasma membrane and extracellular space to the vacuole. Cargo progresses from early endosomes to late endosomes (multivesicular bodies) before reaching the vacuole. In macroautophagy, vesicles called autophagosomes engulf cytosolic material for degradation at the vacuole.
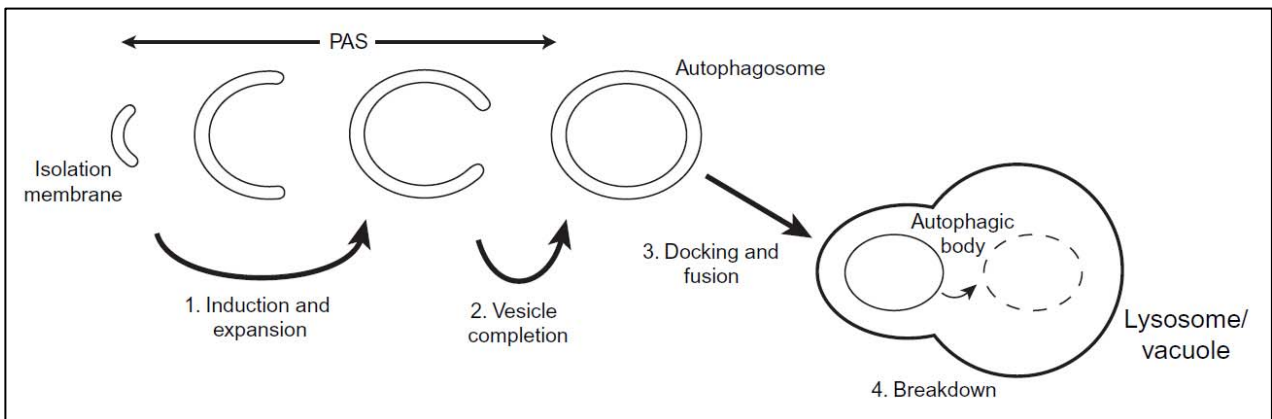
Figure 2. Conceptual model for autophagy.

The basic mechanism of autophagy is the sequestration of the cargo material (bulk cytoplasm, protein aggregates, and, organelles) by a cytosolic double-membrane vesicle (*i.e.,* autophagosome). Various types of stimuli trigger the expansion of the isolation membrane (*step 1*). Upon vesicle completion (*step 2*), the autophagosome docks with the lysosomes/vacuoles and successively fuses with it (*step 3*). In this way, the inner vesicle (*i.e.,* autophagic body), is liberated inside the vacuole, where it is finally consumed together with the cargo by vacuolar hydrolases (*step 4*). Pre-autophagosomal structure (PAS) has been used to describe all the autophagosomal intermediates.
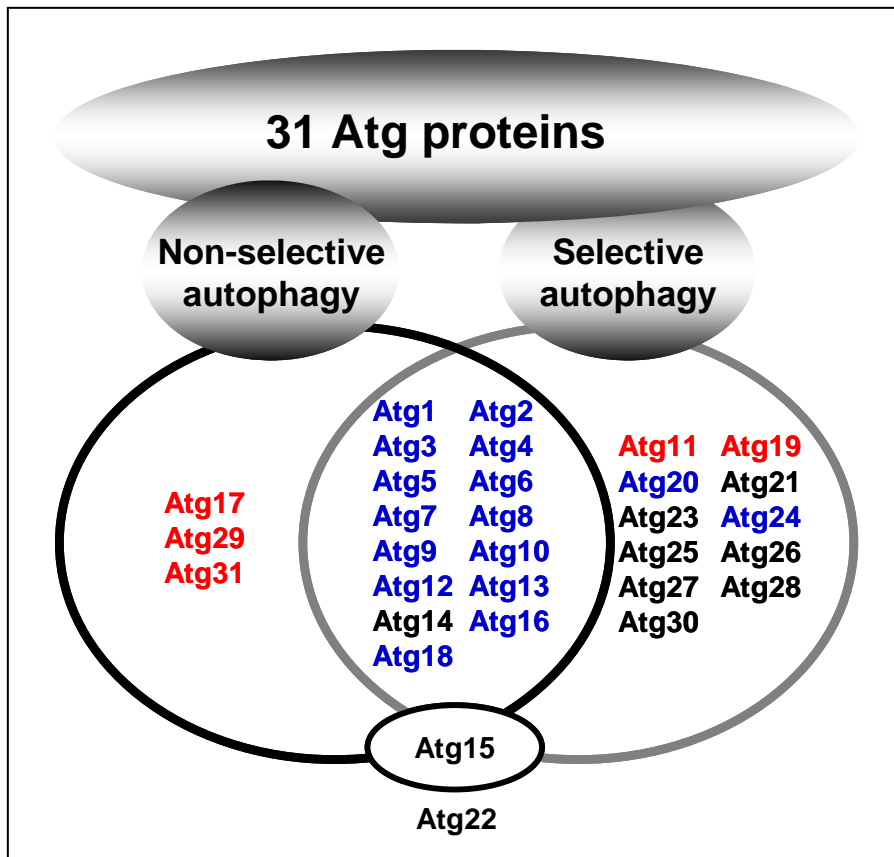
Figure 3. The classification of Atg proteins.

The 31 known Atg proteins are sub-grouped based on their essential function in either nonselective or selective types of autophagy (*see Figure 6*). Eighteen of them are required for both types of autophagy. Conserved Atg proteins are in blue. Atg22 has not been included in this graph because its role in autophagy is controversial. Atg15 is the only Atg protein not involved in the biogenesis of autophagosomes; it participates in the breakdown of autophagic bodies. Atg17, Atg29, and Atg31 are specific factors for (macro)autophagy in yeast. In addition, Atg11 and Atg19 are essential for the Cvt pathway (*see Figure 5*).
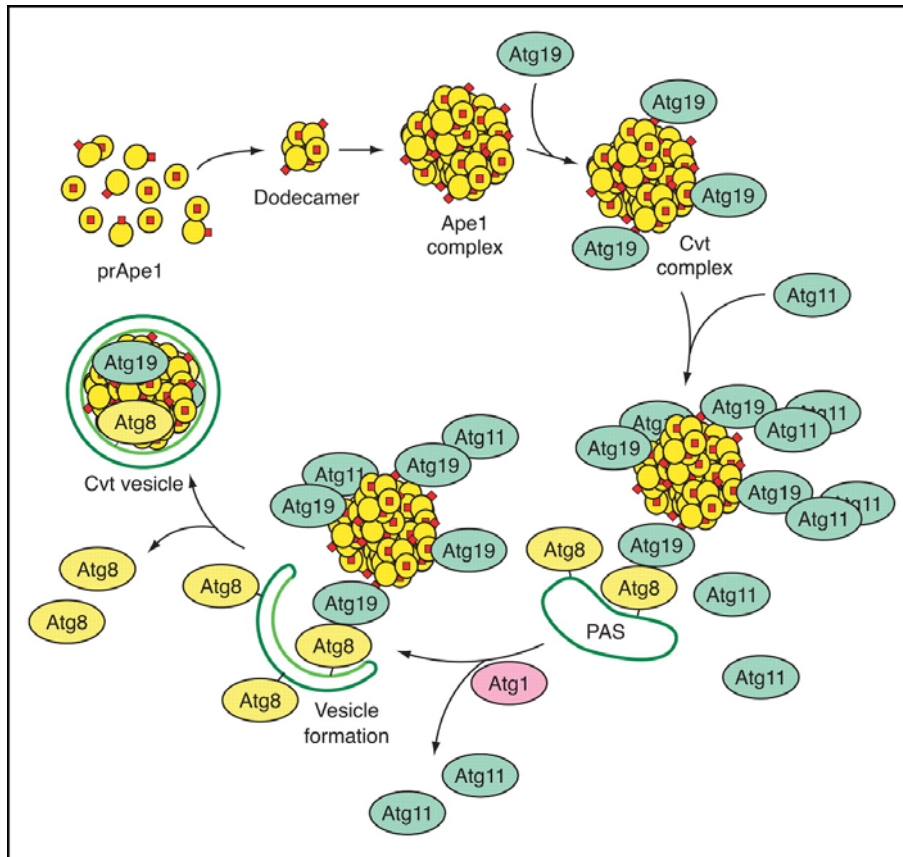
Figure 4. Temporal order for packing cargo components in the Cvt pathway.

Precursor Ape1 monomers assemble into dodecamers and then into a large Ape1 complex. The receptor protein Atg19 binds to the propeptide of prApe1 to generate the Cvt complex. The binding of Atg11 is necessary for this complex to be targeted to the PAS where the disassembly of Atg11 oligomers occurs. Consequently, Atg8 conjugated to phosphatidylethanolamine binds to Atg19 and also to the growing membrane. In the final step of vesicle formation, Atg8–PE that is not enclosed within the vesicle is cleaved by the action of Atg4 (not shown) and released from the outer membrane.
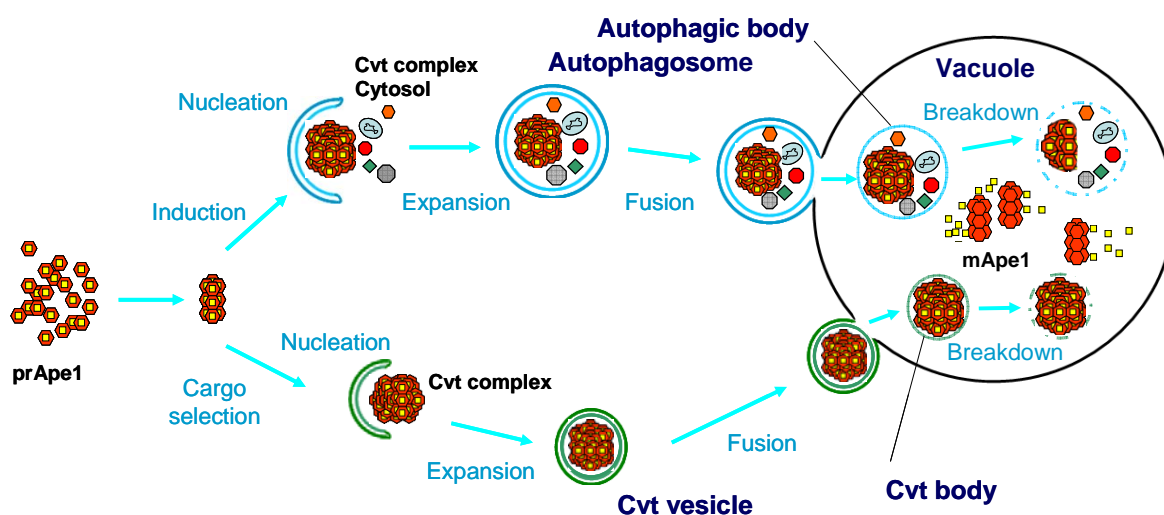
Figure 5.   Schematic representation of autophagy and the Cvt pathway in yeast.

In both autophagy (*upper model*) and the Cvt pathway (*lower model*), cargoes are engulfed by double membrane vesicles. During autophagy, various cytoplasmic components such as organelles and cytoplasm are sequestered into a large, double membrane autophagosome that is 300-900 nm in diameter. The Cvt pathway occurs during vegetative conditions; it is a biosynthetic pathway used to deliver the inactive form of the resident hydrolase aminopeptidase 1 (Ape1) to the vacuole. The Cvt vesicle ranges from 140-160 nm in diameter and, in contrast to the autophagosome, appears to exclude bulk cytoplasm. Following completion, the outer membrane of the sequestering vesicle fuses with the vacuolar membrane. The inner vesicle along with its contents is released into the vacuolar lumen where the vesicle membrane is degraded, allowing processing and activation of prApe1. Under starvation conditions, prApe1 is packaged into autophagosomes and is transported to the vacuole along with other cargo.
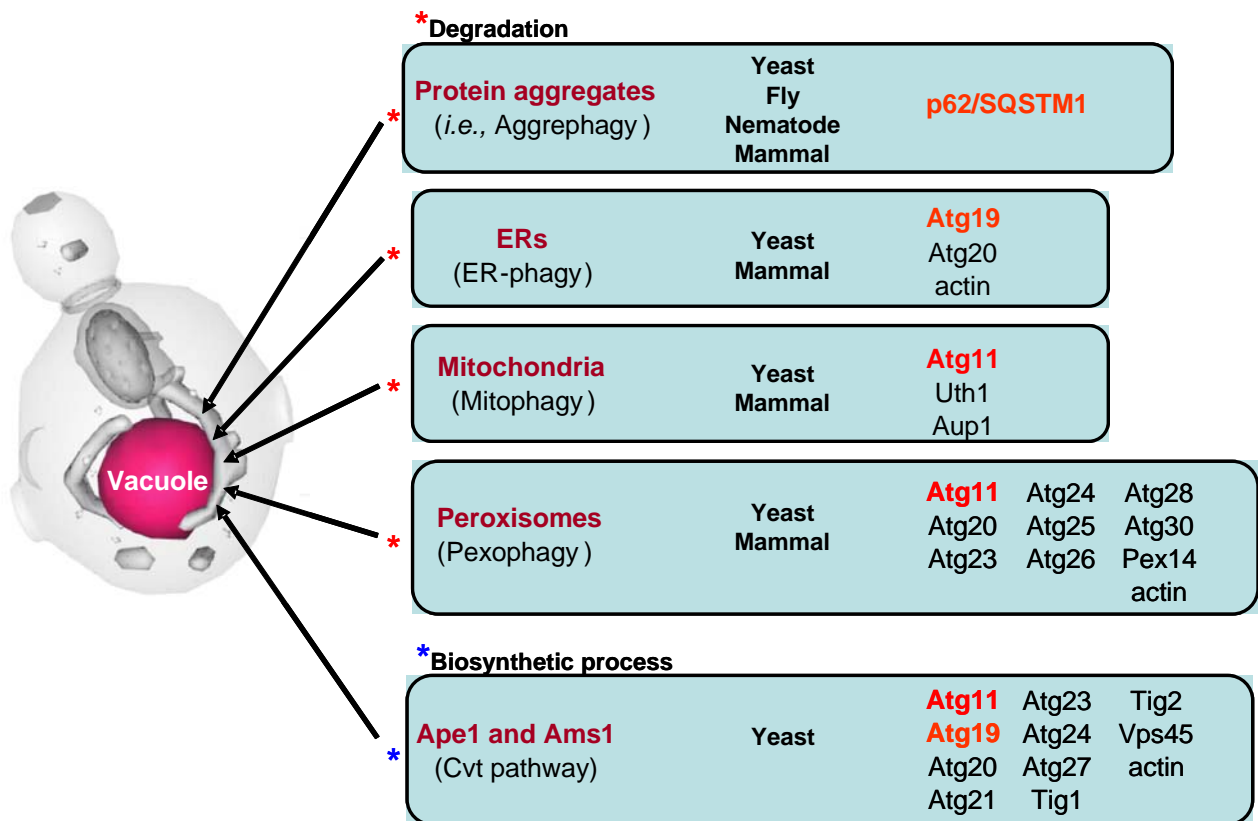
Figure 6.   Selective types of autophagy.

   Cytoplasmic constituents are selectively transported to the vacuole under the various conditions. Red-asterisk groups are transported to the vacuole for degradation. In contrast to reds, blue-asterisk group is selectively transported to the vacuole as a biosynthetic process; Ape1 and Ams1 are vacuole-resident enzymes.
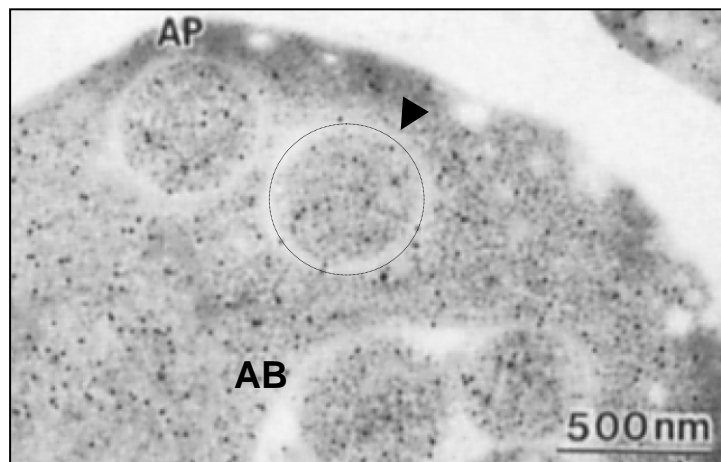
Figure 7. Immunostaining image of alcohol dehydrogenase in yeast cells.

Vacuolar hydrolase deficient cell (*pep4Δ*) contains autophagic bodies in the vacuole and autophagosomes in cytosol (Baba et al., 1994). AP, autophagosome (arrow head and circle); AB, autophagic bodies. Bar, 500 nm.

MATERIALS AND METHODS

1. *Cultivation and Handling of Yeast Strains*

Standard techniques were used for yeast manipulation (Suzuki et al., 2007). The yeast strains used in this study are listed in Table I. Prior to experiments, all strains were grown in YPD medium (1% yeast extract, 2% polypeptone, and 2% glucose) and in YPGly medium (1% yeast extract, 2% polypeptone, and 3% glycerol) (Sherman et al., 1991) supplemented with 0.004% adenine sulfate. Since cells were grown in YPGly medium, single colonies were cultured in YPD medium until logarithmic phase ($A_{600} = 1.0$) and inoculated in YPGly medium at 0.08 unit of A_{600} followed by incubation at 30°C in a temperature-controlled dry shaker orbiting at 210 rpm. After cultured in YPGly medium until early logarithmic phase ($A_{600} = 0.5$) of growth, cells were inoculated in YPGly medium again at 0.08 unit of A_{600} and this operation was repeated for 3 times. For nitrogen starvation, SD-N medium (0.17% yeast nitrogen base without ammonium sulfate and amino acids and with 2% glucose) was used.

2. *Manipulation of Yeast Strains*

The W303-1A strain was transformed with a DNA fragment containing the wild-type *ADE2* open reading frame to produce a parental strain (TKY51). A PCR-based gene modification method (Longtine et al., 1998) was used to disrupt *ATG* genes. Genome DNA extracts from the lab stock were used as the PCR templates. The yeast leucine aminopeptidase III (Lap3) were endogenously tagged with green fluorescent protein (GFP) at the N-terminus by the PCR-based epitope-tagging strategy (Janke et al., 2004). The sequence encoding the *GPD* promoter and the GFP was amplified with the S1 and S4 primer pair from the pYM-N17 plasmid (Janke et al., 2004). In the resulting strain, the endogenous promoter is replaced with a GPD promoter, and the GFP tag is fused to the N-terminus of the Lap3. The $atg1^{ts}$ allele (Suzuki et al., 2001) was integrated in TKY71 strains. The TKY109 and TKY110 strains were generated by transforming the TKY71 and TKY72 cells with pPS129 digested with AvrII (Stromhaug et al., 2004) (plasmid was a gift from Dr. Daniel J. Klionsky, University of Michigan, USA).

3. *Antibodies*

Lap3 specific antibodies were prepared as follow. To raise an antiserum against Lap3, I used synthetic peptides corresponding to amino acids 6-20 and 204-217 as antigens (the NIBB Center for Analytical Instruments, Okazaki, Japan). KLH (Keyhole-Limpet-Hemocyanin) -conjugated peptides were used to immunize rabbits (Shibayagi, Japan). An anti-Ape1

antiserum was described previously (Suzuki and Ohsumi, 2007). An anti-PGK and anti-FLAG antibodies, and an anti-GFP antiserum were purchased from Invitrogen.

4. *Immunoblotting Analysis*

Whole cell lysates were prepared by NaOH/2-mercaptoethanol extraction with a slight modification (Horvath *et al.*, 1994) and by disrupting cells with glass beads in lysis buffer (50 mM Tris-HCl, pH 8.0, 4 mM pephabloch^{TM} and protease inhibitor cocktail, RocheApplied Science). Cells lysates were boiled with SDS-sample buffer for 5 min, and these proteins content was determined by BCA assay kit (Pierce). Total protein (10 μg) was subjected to SDS-PAGE (Suzuki et al., 2007), and transferred to polyvinylidene fluoride membrane (Immobilion^{TM}-P, Millipore) and detected with a combination of each antibody and peroxidase-conyugated goat anti-rabbit IgG antibody (Jackson) or peroxidase-conyugated goat anti-mouse IgG antibody (Jackson) by the ECL system (Parkinelmer). To examine GFP–Lap3 transport, cells were grown in YPD medium to mid-log phase at 30°C, washed in water two times and then incubated in nitrogen starvation medium (SD-N) at 30°C. To monitor stability of Lap3 in the vacuole, cells harboring the *atg1^{ts}* allele were cultured in YPD medium to mid-log phase at 23°C. For starvation, cells were washed in water two times, cultured in SD-N medium at 23°C for 5 h, and then incubated at 37°C to block autophagy. At the time points indicated, 1 ml of culture was harvested and used to prepare cell extract. Protein extracts were subjected to SDS-PAGE as described (Suzuki et al., 2007) and were probed with anti-Lap3, anti-Ape1, anti-GFP and anti-Pgk1 antisera or antibodies.

5. *Microscopy*

Fluorescence microscopy was performed using a TIR-FM system (OLYMPUS) as described (Suzuki et al., 2007). This system was equipped with a 100× objective lens (Apo100 x OHR, NA: 1.65) and a CoolSNAP HQ CCD camera (Nippon Roper). GFP was excited with a mercury lamp and a U-MGFPHQ filter set. For cells labeled with both GFP and RFP, a blue laser (Sapphire 488-20, Coherent) and a yellow laser (85-YCA-010, Melles Griot) were used. A U-MNIBA2, from which the excitation filter was removed, was used for GFP visualization, and an FF593-Di02 dichroic mirror and an FF593-Em02 excitation filter (Semrock) were used to analyze RFP. A UPlanSApo100 x Oil (NA: 1.40) objective lens was used for microscopic observation. Images were acquired using MetaMorph software (Molecular Devices).

6. *Alkaline phosphatase (ALP) assay*

ALP assay was performed as a described previously (Noda et al., 1995). Cells grown to

mid-log phase in YPD (approximately 5 OD_{600} unit) were transferred to SD-N medium for 5 h. Cells grown in YPD were shift to YPGly medium to mid-log phase ($OD_{600} = 0.5$: approximately 4 OD_{600} unit). Cells were collected, and resuspended pellets in 200 μl ice-cold assay buffer (250 μM Tris-Cl, pH 9.0, 10 mM $MgSO_4$, 10 mM $ZnSO_4$, and 4 mM Pephablock^{TM}). An equal volume of (approximately 100 μl) acid-washed glass beads (about 0.5 mm) was added, then cells were lysed by vortexing at 4°C, and the lysates was clarified by centrifugation at 15,000 xg for 5 min. 10 ml aliquot of cell extracts was mixed with 490 μl cold assay buffer. 55 mM alpha-naphythl phosphate was added to start the reaction, and incubated 10 min at 30°C before terminating the reaction by adding 500 μl of stop buffer (2M Glycine-NaOH, pH 11.0). Evaluation of phosphatase activity was monitored by measuring fluorescence (excitation at 345 nm and emission at 472 nm) by spectrophotometer (Hitachi). Protein concentration in the extracts was measured with BCA protein assay kit (Pierce, MA) to normalize the ALP activity. ALP activity was calculated using the following formula*:

1 unit = absorbance / 10.7 x [protein concentration (mg)] x [incubation time (min)]

7. *Vacuole isolation*

   The procedure used previously for preparing pure vacuolar membrane vesicles (Uchida et al., 1985) was modified for use on a large scale. Exponentially growing cells (10 liters, 1 x 10^7 cells/ml) were harvested by centrifugation at 4500 xg for 3 min, washed twice with distilled water at room temperature, and suspended in 1.4 M sorbitol at a density of 2 x 10^7 cells/ml. To this suspension, Zymolyase 100T (Seikagaku) was added to a final concentration of 1 unit/ml, and the mixture was incubated at 30°C for 30 min with gentle shaking. This treatment converted most (>85%) of the cells to spheroplasts, which were then recovered by centrifugation and washed twice with 1.4 M sorbitol with centrifugation (2200 xg, 5 min). The pellet was suspended in about 10 volumes of Buffer A (10 mM Mes/Tris, pH 6.9, 0.1 mM $MgCl_2$, 12% Ficoll 400), homogenized in a loosely fitting dounce homogenizer, and centrifuged in a swinging bucket rotor at 4500 xg for 10 min. For isolation of vacuoles, 20 ml volumes of supernatant were transferred to centrifuge tubes and 10 ml of Buffer A was layered on top. The tubes were centrifuged in a swinging bucket rotor RPS27-2 of a Hitachi model 70P centrifuge at 51,900 xg for 30 min at 4°C. The white layer on top of the tubes, which contained most of the vacuoles, was collected and resuspended in Buffer A with a homogenizer. Then, 15 ml of Buffer B (10 mM Mes/Tris, pH 6.9, 0.5 mM $MgCl_2$, 8% Ficoll 400) was layered on top. After re-centrifugation under the conditions described above, the vacuoles were recovered from the top of the tubes almost free from contaminating lipid granules and other membranous organelles. The vacuoles thus obtained were converted to vacuolar membrane vesicles by

diluting them first with an equal volume of double concentration Buffer C (10 mM Mes/Tris, pH 6.9, 5 mM $MgCl_2$) and then with 2 volumes of Buffer C. The vesicles were recovered by centrifugation at 15,000 xg for 20 min.

8. *Peptide Mass Finger-printing (PMF)*

Vacuole isolation was performed. Protein concentration was measured using BCA protein assay kit (Pierce, MA). Samples including approximately 25 µg protein were used for SDS-PAGE and then stained using Silver stain MS kit (Wako, VA). The protein bands on SDS-PAGE gel (12% acrylamide concentration) were picked. Bands washed with 100 mM ammonium bicarbonate, dehydrated with acetonitrile, and dried in an evaporator. The gel pieces were digested with 0.5 mg/ml of trypsin (trypsin gold, Promega) with 100 mM ammonium bicarbonate for 16 h at 37°C. Digested peptides were extracted from the gel with 10% formic acid and 50% acetonitrile, and were desalted with the ZipTip^{TM} C-18 (Millipore). The samples and a-cyano-4-hydroxy-cinnamic acid (Fluka) were mixed at a 2:1 ratio and were analyzed by matrix associated laser deionization-time of fright (MALDI-TOF) mass spectrometry, REFLEX III (bruker). Proteins were identified by searching the MASCOT, and NCBInr database using MS-Fit program on Protein Prospector

9. *Immunoprecipitation*

Immunopricipitation of GFP–Lap3 and Atg19-FLAG was performed with a slight modification (Denic et al., 2006). Cells were grown to early mid-log phase in YPD (100 OD_{600} units), shifted to YPGly medium (100 OD_{600} units) (The strains in Figure 28 were grown), and harvested by centrifugation. The cells were washed with water, resuspended in 50 ml of D buffer (100 mM Tris-Cl, pH 9.4) containing 5 µM DTT, and incubated for 5 min at room temperature. The cells were pelleted and were converted to spheroplasts. The spheroplasts were pelleted at 700 xg for 5 min at 4°C and the pellet was resuspended in 1.5 ml of cold IP buffer (25 mM HEPES-KOH, pH 6.8, 10 mM NaCl, 1 M sorbitol, 150 mM KOAc, 2 mM MgOAc, 1 mM $CaCl_2$, 1% NP-40, protease inhibitors). The cells were then incubated for 10 min on ice and were lysed by douncing. The lysates were cleared twice at 700 xg for 5 min and the resulting supernatant was subjected to centrifugation at 15,000 xg for 10 min to remove the cell debris. Protein concentration was estimated using a BCA protein assay kit (Pierce, MA). Cell lysates (1-4 mg) were brought up to 1 ml with IP buffer and were incubated with 1-2 µl of anti-GFP and anti-FLAG anti bodies for 1.5 h at 4°C with gentle rotation. The extract/antibody mixture was added 20 ml of 50% slurry of protein G-Spharose 4 FF (GE), followed by a further rotation for 1.5 h at 4°C. After centrifugation 15,000 xg for 1 min, immunocomplex were washed three

times with 1 ml IP buffer. Protein bound to the beads were suspended in sample buffer (100 mM Tris-Cl, pH 6.8, 4% SDS, 20% Glycerol, 0.4% BPB, 200 mM DTT), boiled at 95°C for 4 min, and subject to immunoblot.

10. *Yeast Two-hybrid Analysis*

Two-hybrid assays were carried out essentially as previously described (James et al., 1996). Briefly, pGAD-based and pGBD-based plasmids were co-transformed into the host strain PJ69-4a or its derivatives. Colonies were replica-plated onto either SC (-Trp-Leu-His) containing 3 mM 3 AT or SC (-Trp-Leu-Ade) and testing for growth.

11. *World-Wide-Web Databases*
 a. SGD: Saccharomyces Genome Database
        http://www.yeastgenome.org/
 b. MEROPS: Peptidases database
        http://merops.sanger.ac.uk/
 c. MASCOT: PMF database
        http://www.matrixscience.com/
 d. NCBInr: PMF database
        http://prospector.ucsf.edu

12. *References*

Denic, V., E.M. Quan, and J.S. Weissman. 2006. A luminal surveillance complex that selects misfolded glycoproteins for ER-associated degradation. *Cell*. 126:349-59.

James, P., J. Halladay, and E.A. Craig. 1996. Genomic libraries and a host strain designed for highly efficient two-hybrid selection in yeast. *Genetics*. 144:1425-36.

Janke, C., M.M. Magiera, N. Rathfelder, C. Taxis, S. Reber, H. Maekawa, A. Moreno-Borchart, G. Doenges, E. Schwob, E. Schiebel, and M. Knop. 2004. A versatile toolbox for PCR-based tagging of yeast genes: new fluorescent proteins, more markers and promoter substitution cassettes. *Yeast*. 21:947-62.

Longtine, M.S., A. McKenzie, 3rd, D.J. Demarini, N.G. Shah, A. Wach, A. Brachat, P. Philippsen, and J.R. Pringle. 1998. Additional modules for versatile and economical PCR-based gene deletion and modification in Saccharomyces cerevisiae. *Yeast*. 14:953-61.

Noda, T., A. Matsuura, Y. Wada, and Y. Ohsumi. 1995. Novel system for monitoring autophagy in the yeast *Saccharomyces cerevisiae. Biochem. Biophys. Res. Commun.* 210:126-32.

Sherman, K.A., G.E. Gibson, P. Perrino, and K. Garrett. 1991. Acetylcholine formation from glucose following acute choline supplementation. *Neurochem Res*. 16:1009-15.

Stromhaug, P.E., F. Reggiori, J. Guan, C.W. Wang, and D.J. Klionsky. 2004. Atg21 is a phosphoinositide binding protein required for efficient lipidation and localization of Atg8 during uptake of aminopeptidase I by selective autophagy. *Mol. Biol. Cell*. 15:3553-66.

Suzuki, K., T. Kirisako, Y. Kamada, N. Mizushima, T. Noda, and Y. Ohsumi. 2001. The pre-autophagosomal structure organized by concerted functions of APG genes is essential for autophagosome formation. *EMBO J.* 20:5971-81.

Suzuki, K., Y. Kubota, T. Sekito, and Y. Ohsumi. 2007. Hierarchy of Atg proteins in pre-autophagosomal structure organization. *Genes Cells*. 12:209-18.

Suzuki, K., and Y. Ohsumi. 2007. Molecular machinery of autophagosome formation in yeast, *Saccharomyces cerevisiae*. *FEBS Lett.* 581:2156-61.

Uchida, E., Y. Ohsumi, and Y. Anraku. 1985. Purification and properties of H^+-translocating, Mg^{2+}-adenosine triphosphatase from vacuolar membranes of *Saccharomyces cerevisiae*. *J Biol Chem*. 260:1090-5.

Table I. **Yeast strains used in this study**

Strain	Genotype	Source
W303-1A	*MATα ade2 his3 leu2 trp1 ura3 can1*	Laboratory stock
TKY51	W303-1A; *ADE2*	This study
TKY44	TKY71; *vps20Δ::kanMX*	This study
TKY45	TKY44; *atg7Δ::HIS5*	This study
TKY46	TKY51; *pep4Δ::HIS5*	This study
TKY47	TKY46; *atg7Δ::LEU2*	This study
TKY48	TKY51; *atg7Δ::HIS5*	This study
TKY49	TKY51; *lap3Δ::kanMX*	This study
TKY52	TKY49; *pho8Δ::kanMX-P$_{GPD}$-pho8Δ60*	This study
TKY53	TKY52; *atg7Δ::spHIS5*	This study
TKY81	TKY51; *natNT2-P$_{GPD}$-yeGFP-LAP3*	This study
TKY71	TKY81; *pep4Δ::spHIS5*	This study
TKY72	TKY71; *atg7Δ::LEU2*	This study
TKY73	TKY71; *atg1Δ::kanMX*	This study
TKY74	TKY71; *atg11Δ::kanMX*	This study
TKY75	TKY71; *atg17Δ::URA3*	This study
TKY76	TKY71; *atg19Δ::URA3*	This study
TKY77	TKY71; *atg20Δ::kanMX*	This study
TKY78	TKY71; *atg21Δ::kanMX*	This study
TKY79	TKY71; *atg29Δ::kanMX*	This study
TKY80	TKY71; *atg31Δ::kanMX*	This study
TKY92	TKY71; *ape1Δ::LEU2*	This study
TKY101	TKY51; *yeGFP-LAP3*	This study
TKY102	TKY101; *atg7Δ::LEU2*	This study
TKY103	TKY101; *atg11Δ::kanMX*	This study
TKY104	TKY101; *atg17Δ::URA3*	This study
TKY105	TKY101; *atg19Δ::URA3*	This study
TKY106	TKY101; *ape1Δ::LEU2*	This study
TKY107	TKY101: *mito-RFP::URA3*	This study
TKY108	TKY102; *mRFP-APE1::URA3*	This study
TKY142	TKY51; *ATG19-FLAG-kanMX atg7Δ::HIS5*	This study
TKY109	TKY71; *mRFP1-APE1::URA3*	This study
TKY110	TKY109; *atg7Δ::LEU2*	This study
TKY82	TKY81; *atg1Δ::kanMX*	This study

TKY83	TKY81; *atg7Δ::LEU2*	This study
TKY84	TKY81; *atg11Δ::kanMX*	This study
TKY86	TKY81; *atg19Δ::URA3*	This study
TKY85	TKY81; *atg17Δ::URA3*	This study
TKY89	TKY81; *atg29Δ::URA3*	This study
TKY90	TKY81; *atg31Δ::kanMX*	This study
TKY91	TKY81; *ape1Δ::LEU2*	This study
TKY151	TKY51; *atg1^{ts} ::kanMX*	This study
PJ69-4A	*MATa his3-200 leu2-3, 112 trp1-901 ura3-52 gal4 gal80*	Laboratory stock
	GAL2-ADE2 LYS2::GAL1-HIS3 met2::GAL7-lacZ	

<u>Chapter I</u>

LAP3 IS A SELECTIVE TARGET OF AUTOPHAGY
DURING NITROGEN STARVATION
IN THE YEAST *Saccharomyces cerevisiae*

<u>Chapter I</u>

LAP3 IS A SELECTIVE TARGET OF AUTOPHAGY
DURING NITROGEN STARVATION
IN THE YEAST *Saccharomyces cerevisiae*

Chapter I

Lap3 is a selective target of autophagy during nitrogen starvation

in the yeast *Saccharomyces cerevisiae*

I-A   Backgrounds

I-A-1   *Lap3 and Ape1 Are Self-compartmentalizing Proteins*

Leucine aminopeptidase III (*LAP3*) was originally isolated, along with *LAP1* and *LAP4/APE1*, in a genetic screen (Trumbly and Bradley, 1983). Lap3 (EC 3.4.22.40) is a 454-amino acid multi-functional protein and is conserved among eukaryotes (Berti and Storer, 1995). Moreover, Lap3 is homohexameric protein of approximately 300 kDa. The crystal structures of the yeast and the human enzyme were solved, respectively (Figure 8) (Joshua-Tor et al., 1995; O'Farrell et al., 1999). They are overall very similar to each other and both reveal a hexameric structure with the six identical subunits arranged in a ring (Figure 8*A*; Figure 8*B*), and the monomers have a papain-like polypeptide fold as the core (Figure 8*C*). More recently, Noda and Inagaki solved a crystal structure of Lap4/Ape1 (Noda NN and Inagaki F, unpublished data; Figure 8*D*). Lap4/Ape1 forms a homooligomer of approximately 750 kDa (Kim et al., 1997) and is self-assemble protein similarly to Lap3 (Figure 8*B*).

I-A-2   *Ape1 Is Selectively Transported to the Vacuole during Nitrogen Starvation*

Yeast has a system that selectively transports the vacuole-resident enzymes aminopeptidase I (Ape1/Lap4) and α-mannosidase (Ams1) from the cytoplasm to the vacuole during vegetative growth via the Cvt pathway. The precursor Ape1 (prApe1) and Ams1 are sequestered into the Cvt vesicle (Figure 5) (Baba et al., 1997). Since most of the autophagy-related (*ATG*) genes are required for the vesicle formation, this pathway is an autophagy-related process that encompasses the biosynthetic route of Ape1 and Ams1. During nitrogen starvation, Ape1 and Ams1 are selectively sequestered into autophagosomes (Figure 5). prApe1 is first targeted to the Cvt complex in the cytoplasm (Kim et al., 1997; Oda et al., 1996). Atg19 is a receptor for the Cvt complex (Scott et al., 2001; Shintani et al., 2002), and Atg11 mediates targeting of the Cvt complex to the pre-autophagosomal-structure (PAS), a center of autophagosome formation, by associating with Atg19 (Figure 4) (Yorimitsu and Klionsky, 2005). After the Cvt complex enters the vacuole via an autophagosome, prApe1 is converted to mature Ape1 (mApe1) by vacuolar

hydrolases (Klionsky et al., 1992). In contrast to Atg11 and Atg19, a complex composed of Atg17, Atg29, and Atg31, shows little contribution to Ape1 transport (Kabeya et al., 2007; Kawamata et al., 2008); the complex, however, is required to form normal sized-autophagosomes.

<center>I-B: Results in this chapter</center>

I-B-1   *Lap3 Is Transported to the Vacuole via Autophagosome*

To investigate whether Lap3 is transported to the vacuole similarly to Ape1, I generated a strain expressing GFP–Lap3 from its endogenous promoter and made observations during nitrogen starvation using fluorescence microscopy. As the GFP signals were too weak to be analyzed (data not shown), I generated a cell overexpressing GFP–Lap3 from the *GPD* promoter and made observations using fluorescence microscopy in *pep4Δ* cells. Pep4 is a major vacuolar protease, and Pep4 disruptant prevents a degradation of transported vesicles inside the vacuole. When cells overexpressing GFP–Lap3 were subjected to nitrogen-starvation conditions, a punctate GFP dot was observed next to the vacuole, and GFP dots were transported into the vacuole (Figure 9, *upper panels*). To investigate whether these dots corresponded to autophagic bodies, autophagy was blocked by disrupting *ATG7*. In *pep4Δatg7Δ* cells, GFP dots were not observed inside the vacuole; instead, GFP–Lap3 further accumulated in the punctate dot next to the vacuole (Figure 9, *lower*). These results indicate that Lap3 is transported to the vacuole via autophagosomes. In contrast, during vegetative growth, GFP–Lap3 localized at the cytoplasm, and GFP dots were not observed in the vacuolar lumen (data not shown).

I next assessed Lap3 transport to the vacuole by biochemical approaches. GFP–Atg8 has previously been used to trace the Cvt pathway as well as autophagy (Shintani and Klionsky, 2004; Suzuki et al., 2007). After GFP–Atg8 enters the vacuole, the GFP moiety is cleaved off and accumulates in the vacuolar lumen because it is relatively resistant to proteolysis by vacuolar hydrolases. This GFP monitoring assay is generally applicable to protein transport to the vacuole and has been used to monitor transport of Ape1 (Suzuki et al., 2002), peroxisomes (Reggiori et al., 2005) and mitochondria (Kanki and Klionsky, 2008). To trace the vacuolar transport of Lap3, I generated wild-type, *pep4Δ*, and *atg7Δ* cells expressing GFP–Lap3. Upon transport of GFP–Lap3 to the vacuole, it is exposed to vacuolar hydrolases and is cleaved into GFP (hereafter called v-GFP) and Lap3 (hereafter called v-Lap3). In wild-type cells, v-GFP was not detected during vegetative growth, and a full-length GFP–Lap3 remained stable (Figure 10, *lane 3*). During nitrogen starvation, I detected v-GFP (Figure 10, *lane 4*); this was, however, absent from *pep4Δ* cells, showing that the production of v-GFP depends on vacuolar hydrolases (Figure 10, *lane 5*). In *atg7Δ* cells, v-GFP was not produced (Figure 10, *lane 6*), indicating that Lap3 transport is

dependent on autophagy. These results are consistent with the microscopic observations (Figure 9). I next performed immunoblotting using an antiserum against Lap3 (Figure 10, *middle panel*). During nitrogen starvation, both GFP–Lap3 and v-Lap3 were detected (compare Figure 10, *lanes 3* and *4*). In *pep4Δ* and *atg7Δ* cells, no v-Lap3 was found, but GFP–Lap3 levels were higher (Figure 10, *lanes 5* and *6*), indicating that v-Lap3 is generated from GFP–Lap3 in the vacuole after transport via the autophagosome. This biochemical analysis further supports my conclusion that GFP–Lap3 is transported to the vacuole by autophagy. It is noteworthy that the amount of endogenous Lap3 increases during nitrogen starvation (Figure 10, *lanes 1* and *7*).

In GFP–Lap3 overexpressing cells, Ape1 transport (via the Cvt pathway) was defective during vegetative growth in wild-type cells (compare Figure 10, *lanes 1* and *3*), and this defect was restored by nitrogen starvation (Figure 10, *lanes 4* and *7*). In this strain, autophagic bodies accumulated normally (DIC image of *pep4Δ* in Figure 9), showing that overproduction of GFP–Lap3 does not affect autophagosome formation and fusion with the vacuole. Presumably, PAS targeting of the Cvt complex is normal in this strain, but autophagosome formation is required to encapsulate Ape1. It is reasonable that Ape1 transport was impaired in the *atg7Δ* cells (Figure 10, *lane 6*).

I-B-2 *Lap3 Is Degraded in the Vacuole during Nitrogen Starvation*

I next examined the fate of GFP–Lap3 inside the vacuole; the appearance of v-Lap3 was monitored in wild-type and *atg1Δ* cells. Cells were grown in YPD medium, shifted to nitrogen starvation medium (SD−N) and collected at the indicated time points. Cell lysates were prepared and subjected to immunoblot. In *atg1Δ* cells, the amount of GFP–Lap3 did not change and v-Lap3 never appeared (Figure 11*A*, *lanes 9-16*). In these cells, prApe1 was not converted to mApe1 and consequently prApe1 accumulated during starvation (Figure 11*A*, *lanes 10-16*; Figure 11*B*, *right panel*). In wild-type cells, v-GFP gradually accumulated after shift to SD−N (Figure 11*A*, *lanes 2-8*), showing that the progression of autophagy is correctly monitored. v-Lap3 appeared 0.5 h after shift to starvation medium and was detectable over time (Figure 11*A*, *lanes 2-8*). About 50% of the GFP–Lap3 was converted to v-Lap3 in 1.5 h (Figure 11*B*, left panel); whereas a half-time of prApe1 was about 1 h under the same conditions (Figure 11*B*, right). Scott *et al.* previously showed by [^{35}S]methionine pulse-chase experiments that 27% of Pho8Δ60, an indicator of general cytosolic proteins, was transported to the vacuole within 6 h (Scott et al., 1996). As the rate of Lap3 transport is much higher than that of Pho8Δ60, it is possible that GFP–Lap3 is selectively transported to the vacuole via autophagy.

It is noteworthy that v-Lap3 was apparently reduced during prolonged starvation, whereas mApe1 gradually accumulated (Figure 11*A*, *lanes 2-8*; Figure 11*B*, *right*). This result suggests that

Lap3 is less stable in the vacuole than mApe1. To analyze the kinetics of Lap3 degradation in the vacuole, cells harboring a temperature-sensitive allele of *atg1* (Shintani and Klionsky, 2004 ; Suzuki et al., 2002; Suzuki et al., 2001) were incubated in starvation medium at the permissive temperature (23°C) for 5 h and then shifted to the non-permissive temperature (37°C). Samples were taken at the indicated times and followed by immunoblot. At the non-permissive temperature, prApe1 accumulated because of a block in autophagy (Figure 12*A*), and the amount of mApe1 was relatively constant during the time course (Figure 12*A*, *lanes 2-12*; Figure 12*B*, *closed circle*). GFP–Lap3 also accumulated at the non-permissive temperature, but the amount of v-Lap3 decreased to 50% of its initial level within 1.5 h and was subsequently eliminated (Figure 12*B*, *open circle*). These results indicate that Lap3 is much less stable than mApe1 against vacuolar hydrolases and is degraded in the vacuole.

I-B-3   *Lap3 Localizes to the Cvt Complex*

GFP–Lap3 forms a dot (Figure 9) reminiscent of the Cvt complex labeled with Ape1 (Obara et al., 2008; Stromhaug et al., 2004; Suzuki et al., 2007). When Ape1 transport is prevented by disrupting *ATG* genes, prApe1 accumulates at the Cvt complex and the brightness of Ape1–GFP increases (Suzuki et al., 2002). During nitrogen starvation, GFP–Lap3 exhibited a perivacuolar punctate pattern and almost all dots co-localized with mRFP-Ape1 (Figure 13*A*). Careful observation showed that the GFP–Lap3 and mRFP–Ape1 dots did not merge, but were very close to each other (Figure 13*A*, *inset*). Next, I observed that GFP–Lap3 localized adjacent to mRFP–Ape1 inside the same autophagic bodies in *pep4Δ* cells (Figure 13*B*, *inset*). Since Lap3 and Ape1 very closely localize in the cytoplasm, they can be transported to the vacuole via the same autophagosomes.

I investigated whether Ape1 was required for the transport of Lap3. Ape1 is essential for the delivery of Ams1 to the vacuole during vegetative growth (Shintani and Klionsky, 2004). During nitrogen starvation, in *ape1Δ* cells, v-Lap3 and v-GFP were detected at the same level as in wild-type cells, indicating that Lap3 transport does not require Ape1 (Figure 14, *lanes 2* and *10*). In *ape1Δ* cells as well as wild-type cells, GFP–Lap3 was observed as a punctate dot (data not shown). In *lap3Δ* cells, Ape1 was transported to the vacuole in a normal manner (Figure 10, *lanes 1, 2, 7,* and *8*). Taken together, I conclude that GFP–Lap3 is transported to the vacuole by forming a dot associating with the Cvt complex and can be delivered independently of Ape1.

I-B-4   *Lap3 Is Selectively Transported to the Vacuole by a Similar Mechanism to Ape1*

During nitrogen starvation, Lap3 is transported to the vacuole together with Ape1 (Figure 13*B*); therefore, I next investigated the mechanism of transport. Atg11 and Atg19 play essential

roles in Ape1 transport (Figure 6) (Shintani et al., 2002). In *atg11Δ* and *atg19Δ* cells, Ape1 transport was severely blocked during nitrogen starvation (compare *lanes 2*, *5*, and *6* in Figure 14). In these cells, the amounts of v-Lap3 and v-GFP decreased relative to wild-type cells (Figure 14, *lanes 5* and *6*), indicating that Atg11 and Atg19 are important for GFP–Lap3 transport. I thus conclude that Lap3 is selectively transported to the vacuole using similar mechanisms to Ape1.

Atg17 is necessary for autophagosome formation and acts as a heteromeric complex containing Atg29 and Atg31 (Kawamata et al., 2008). In *atg17Δ*, *atg29Δ*, and *atg31Δ* cells, Ape1 transport is not impaired (Kabeya et al., 2007). I examined Ape1 transport in GFP–Lap3 overexpressing cells during vegetative growth. Transport seemed normal in *atg17Δ* cells (compare *lanes 2* and *7* in Figure 15), whereas it was defective in *atg29Δ* and *atg31Δ* cells (Figure 15, *lanes 8* and *9*). During nitrogen starvation, transport was slightly defective in *atg17Δ* cells, and was severely impaired in *atg29Δ* and *atg31Δ* cells (Figure 14, *lanes 7-9*). Next, I examined GFP–Lap3 transport. The amount of v-GFP was severely decreased in these *atg17Δ*, *atg29Δ*, and *atg31Δ* disruptants, similar to Ape1 transport (Figure 14, *lanes 7-9*). Probably, normal autophagosome formation is required for both Lap3 and Ape1 transport in GFP–Lap3 overexpressing strains.

I-C   Discussion

I analyzed in this chapter whether Lap3 was transported to the vacuole under nitrogen-starvation conditions using GFP-fused Lap3. The overexpressed GFP–Lap3 is not delivered to the vacuole during vegetative growth, but is during nitrogen starvation, indicating that nitrogen-starvation stimulates GFP–Lap3 transport. This may be because autophagosomes have much greater capacity than Cvt vesicles or because starvation targets GFP–Lap3 to autophagosomes. Autophagy has traditionally been described as a non-selective degradation process. Onodera and Ohsumi previously reported that Ald6, a cytosolic aldehyde dehydrogenase, is preferentially sequestered in autophagosomes (Onodera and Ohsumi, 2004), indicating that Ald6 is a selective target of autophagy. I showed that the rate of Lap3 transport was much higher than that of Ald6 (Figure 11*A*). Approximately 90% of the GFP–Lap3 was converted to v-Lap3 in 5 h (Figure 11*B*); the amount of Ald6, however, was not reduced after 5-h starvation in wild-type cells, suggesting that Lap3 is more effectively sequestered into autophagosomes than Ald6. I demonstrated that Lap3 was transported to the vacuole using similar mechanisms to Ape1 and was degraded in the vacuole, whereas Atg11 and Atg19 are not involved in Ald6 reduction (Onodera and Ohsumi, 2004). I conclude that Lap3 is a novel target of selective autophagy.

When GFP–Lap3 is overexpressed, it forms a dot structure and is spatially associated with the Cvt complex during vegetative growth and during nitrogen starvation (Figure 13). Why does Lap3

accumulate at the Cvt complex under the conditions? In mammalians cells, protein-aggregate formation is a pathological feature of diseases including Parkinson's, Alzheimer's, and Huntington's diseases (Rubinsztein, 2006; van der Vaart et al., 2008). Polyubiquitinated aggregates are recognized by p62, selectively sequestered by autophagosomes and degraded in lysosomes (Ichimura et al., 2008; Komatsu et al., 2007; Pankiv et al., 2007). This process is thought to be crucial for survival of mammalian cells. I do not know yet whether GFP–Lap3 dots are harmful or disadvantageous for yeast cells. The analysis of mechanism(s) for that Lap3 accumulates into the Cvt complex may help to understand the mechanisms that eliminate protein aggregates in eukaryotic cells.

Chapter II

MACHINERY OF THE CVT PATHWAY ACTS FOR DEGRADATION
DURING GLYCEROL GROWTH
IN THE YEAST *Saccharomyces cerevisiae*

RESULTS

Chapter II

Machinery of the Cvt pathway acts for degradation during YPGly growth
in the yeast *Saccharomyces cerevisiae*

II-A   Backgrounds

II-A-1   *Yeast Grows in a Medium Containing Fermentable and Non-Fermentable Carbon Sources*

The yeast *Saccharomyces cerevisiae* (hereafter simply called yeast) adapts to a wide variety of growth conditions in response to its extracellular environments, and yeast has an ability to utilize different carbon sources. To adapt the various carbon sources, transcriptional patterns and cell metabolisms are drastically changed. Glucose is a fermentative carbon source for the yeast; *e.g.*, in the presence of this sugar, yeast metabolism is primarily fermentative, and the product of the process is ethanol. Under the conditions, yeast does not need fully active mitochondria because sufficient energy is provided by glycolysis and fermentation. In contrast to glucose, the metabolism of non-fermentable carbon source such as acetate, glycerol, and ethanol requires mitochondrial function. Furthermore, expression of the mitochondrial ribosomal proteins (MRP) genes is induced and exhibits the relatively slow growth (Rolland et al., 2002).

II-A-2   *Studies on Yeast Autophagy under Catabolite-repressed Conditions*

To date, studies on yeast autophagy have been performed using *S. cerevisiae* cultured in a medium containing glucose (YPD). Glucose is the preferred carbon source for yeast, and cells growing in a medium containing only this sugar repress expression of genes encoding products required for metabolism of other carbon sources; this is referred to "glucose repression" or "catabolite repression" (Carlson et al., 1999; Gancedo, 1998; Rolland et al., 2002). Other sugars, such as raffinose, glycerol, galactose, or maltose, are able to affect the synthesis of enzymes repressed by glucose.

Hansen *et al*. previously described (Hansen et al., 1977) that activity of vacuolar hydrolases in cells grown with acetate are 3-10 times higher than that in cells grown with glucose. Moreover, two groups reported by the global gene expression studies that mRNA encoding vacuole-resident enzymes were increased after a shift from YPD to a medium containing glycerol (YPGly) (Kuhn et al., 2001; Roberts and Hudson, 2006). In this chapter, I show that autophagy occurs constitutively during vegetative growth on non-fermentable media.

II-B   Results in this chapter

II-B-1   *The Vacuolar Transport Pathway Enhances during YPGly Growth*

I biochemically assessed the amount of vacuolar enzymes in YPD and YPGly grown cells (Figure 16). Total lysates were prepared from cells grown to the logarithmic phase ($A_{600} = 0.4\text{-}0.5$; Figure 17) in YPD and YPGly media, respectively and subjected to immunoblot. Prb1 and Prc1, which are major vacuole-resident enzymes, are transported into the vacuole by the vacuolar-protein-sorting (Vps) pathway (Piper et al., 1995). Expression of Prb1 and Prc1 was up-regulated in YPGly grown cells compared to that in YPD grown cells (Figure 16, *lane 2*), suggesting that the activity of the Vps pathway is enhanced during YPGly growth. These results are consistent with reported microarray-based analyses (Kuhn et al., 2001; Roberts and Hudson, 2006).

Hutchins *et al*. previously described that the level of α-mannosidase (Ams1), which is a cargo of the Cvt pathway, increased, and Ams1 transport was detected after cells shifted from glucose medium to glycerol medium (Hutchins and Klionsky, 2001). The amount of aminopeptidase I (Ape1) was also increased in YPGly grown cells (Figure 16, *lanes 1* and *2*). These results suggest that the transport level is up-regulated during YPGly growth; the Cvt pathway enhanced under the conditions. Indeed, the level of Atg8 and PE-conjugated Atg8 (Atg8–PE), which are indicators for formation of the Cvt vesicles and/or autophagosomes (Abeliovich et al., 2000), were enhanced in YPGly grown cells (Figure 16, *lane 2*). Elevated activities of vacuolar transport suggest an increase of lytic function of the vacuole during YPGly growth; this may be important for YPGly grown cells.

II-B-2   *Intravacuolar Structures Accumulate in pep4Δ Cells during YPGly Growth*

Under nitrogen-starvation conditions, autophagic bodies are observed inside the vacuole of *pep4Δ* cell (*Chapter I*). I observed autophagic body like-structures in the vacuole during YPGly growth (Figure 18, *right panel*), whereas no intravacuolar structures were observed in YPD grown cells by light microscopy (Figure 18, *left*). To characterize the structures, I performed the following observation in *pep4Δ*-based mutants during YPGly growth.

The multivesicular bodies are formed by an invagination of the late endosomal membrane (Bryant and Stevens, 1998). After the late endosome fused to the vacuole membrane, the invaginated vesicles into late endosome were transferred and accumulated in the vacuole of *pep4Δ* cells during growth conditions (Reggiori et al., 2000). Vps20 is required for the multivesicular body formation. In *pep4Δvps20Δ* cells, the numbers of the intravacuolar structures decreased (Figure 19*A*, *left panel*). I next investigated whether the remained structures in the vacuole

corresponded to autophagic bodies; autophagic process is blocked by disrupting *ATG7*. The intravacuolar structures were completely disappeared in *pep4Δvps20Δatg7Δ* cells (Figure 19*A*, *right*), indicating that major part of intravacuolar structures is *ATG7*-dependent vesicles and derived from autophagic process.

II-B-3   *Non-Selective Autophagy Is Undetectable under YPGly Growth Conditions*

To characterize the intravacuolar structures in YPGly grown cells, I performed electron microscopy (Figure 19*B*). In *pep4Δ* cells, the various vesicles were detected in the vacuole (Figure 19*B*, *panels a* and *b*). *pep4Δatg7Δ* cells accumulated 40-50 nm vesicles inside the vacuole (Figure 19*B*, *panel c*), which are similar to the reported multivesicular bodies in size (Reggiori and Pelham, 2001). In *pep4Δvps20Δatg7Δ* cells, intravacuolar structures were not detected completely (Figure 19*B*, *panel d*). These observations are consistent with the foregoing light microscopy (Figure 19*A*). Interestingly, *ATG7*-dependent structures had a size of approximately 200-300 nm in diameter (Figure 19*B*, *panels a* and *b*). Since intravacuolar structures during nitrogen starvation have a size of 500-900 nm (Figure 7) (Baba et al., 1994), the structures may be not autophagic bodies. Moreover, the ribosomes and membranes seemed to be excluded from these structures

I next examined biochemically whether autophagy occurs in YPGly grown cells, an alkaline phosphatase (ALP) assay was applied (Figure 20) (Noda et al., 1995). The ALP assay monitors the transport of cytoplasm into the vacuole via autophagy by measuring the activity of alkaline phosphatase that is artificially expressed in the cytosol as a precursor form and transported into the vacuole via autophagy, where it is converted to the mature form. I obtained the deletion mutant for *ATG7* and its isogenic wild-type parent strain overexpressing Pho8Δ60, respectively. ALP assay was performed using lysates prepared from wild-type and *atg7Δ* cells grown in YPGly to the logarithmic phase (A_{600} = 0.4-0.5; Figure 21). As shown in Figure 20, there was no significant difference in its activity between wild-type and *atg7Δ* cells, providing evidence that autophagic activity is undetectable, if any, during YPGly growth; Therefore, these results show that non-selective autophagy is not induced during YPGly grown cells.

II-B-4   *Identification of Enwrapped Proteins in the Intravacuolar Structures*

To identify the proteins contained in the *ATG7*-dependent vesicles, I isolated vacuoles from *pep4Δ* cells with or without *ATG7* gene (Figure 22*A*) and subjected to proteomic analysis. The vacuoles were isolated and purity of the fraction was assessed by immunoblot using organelle markers (Figure 22*A*). The soluble vacuolar enzymes Ape1 and Prc1, and the vacuole membrane protein Pho8 were enriched in this fraction (Figure 22*A*, *lanes 3* and *4*); while the cytosolic enzyme Pgk1 was largely excluded (Figure 22*A*, *lanes 1-4*). Marker proteins, moreover, which are

the endoplasmic reticulum (Dpm1), the Golgi (Sed5), and the mitochondria (Tom70), were not detected (Figure 22*A*, *lanes 1-4*).

The total vacuole fraction was subjected to SDS-PAGE, and proteins were visualized by silver staining (Figure 22*B*). Several bands detectable only in the vacuole fraction from *pep4Δ* cells were analyzed by mass spectrometry after trypsin treatment (*see "Materials and Methods"*; Figure 23). Leucine aminopeptidase III (Lap3) was detected as an *ATG7*-dependent band in repetitive experiments (Figure 22*B*, *lanes 1* and *2*), indicating that Lap3 is transported from the cytoplasm to the vacuole during YPGly growth. In addition, prApe1 was also identified in this analysis, indicating that proteomic analysis is precisely performed. Although a number of proteins besides Lap3 were identified, they are not clear that are simply contaminants, and not investigated them further. Importantly, Lap3 and Ape1 are the selective targets of autophagy during nitrogen starvation (*Chapter I,* Figure 11).

II-B-5 *Behavior of Lap3 under the Various Growth Conditions*

I performed the immunoblot analysis using antiserum against Lap3 to quantify an endogenous expression of Lap3 (Figure 24*A*). The amount of Lap3 during YPGly growth increased approximately 15 times as compared with that of YPD grown cells (Figure 24*B*). The biochemical characterization of Lap3 in YPD grown cells has hardly been done, probably because of the low expression level of Lap3 (Figure 24*A*, *lane 1*) (Xu and Johnston, 1994; Zheng et al., 1997). I next analyzed the localization of Lap3 using the fluorescence microscope. Cell expressed GFP–Lap3 via its own promoter was observed during YPD and YPGly growth. The localization of GFP–Lap3 was detected in the mitochondria and in cytoplasm during YPD growth (Figure 25, *upper panels*) and verified that GFP–Lap3 was co-localized with mitochondrial marker (*i.e.*, mito–RFP). During YPGly growth, the fluorescence of GFP–Lap3 was enhanced in the cytosol (Figure 25, *lower*), consistent with the immunoblot analysis using antiserum against Lap3. In addition, GFP–Lap3 formed a punctuate dot next to the vacuole (Figure 25, *lower*). Under this conditions, however, Mito–RFP was not accumulated at the punctuate dot.

II-B-6 *Atg19 Acts as a Receptor for Lap3 Transport*

To monitor the vacuolar transport of Lap3, I generated the *pep4Δ* cells expressed GFP–Lap3 from its own promoter and observed using a fluorescence microscope. The GFP signals, however, were not detected in the vacuole lumen during YPGly growth (data not shown). Then, GFP–Lap3 from the GPD promoter was expressed in *pep4Δ* cells. GFP–Lap3 accumulated at a punctuate dot next to the vacuole and the moving GFP positive structures were observed in the vacuole lumen in YPGly grown cells (Figure 26). These signals were not detected in that of the *pep4Δatg7Δ* cells

(Figure 26). I next biochemically traced the vacuolar transport. Wild-type and *atg7Δ* cells overexpressing GFP–Lap3 were subjected to immunoblot with antibody against GFP antiserum (Figure 27); once GFP–Lap3 is transported to the vacuole, GFP–Lap3 is eventually exposed to the vacuolar hydrolases, and is processed into GFP (hereafter called v-GFP) and Lap3 (hereafter called v-Lap3). In *atg7Δ* and *pep4Δ* cells, v-GFP was not detected (Figure 27, *lanes 5-7*), confirming that the GFP–Lap3 was actually transported to the vacuole dependent on *ATG7*.

I examined the mechanism of Lap3 transport using the v-GFP monitoring assay. Atg11 is essential for the Cvt pathway, pexophagy, and mitophagy, in argument with previous reports (Figure 6) (Kanki and Klionsky, 2008; Yorimitsu and Klionsky, 2005) and is not essential for autophagy. In addition, Atg19 functions as a receptor for prApe1 (Shintani and Klionsky, 2004). In *atg11Δ* and *atg19Δ* cells, v-GFP was not detected (Figure 28, *lanes 4* and *6*), indicating that Lap3 was transported to the vacuole via the Cvt pathway during YPGly growth. Under the conditions, Ape1 transport was completely inhibited (Figure 28, *lanes 4* and *6*). In contrast to Atg11, Atg17 is an essential factor for autophagy (Suzuki and Ohsumi, 2007) and acts as a heteromeric complex containing Atg29 and Atg31 (van der Vaart et al., 2008). The amounts of v-GFP and v-Lap3 did not change in *atg17Δ*, *atg29Δ* and *atg31Δ* cells as compared with that of wild-type (Figure 28, *lanes 2* and *5*; Figure 29, *lanes 1-4*).

I hypothesized that Atg19 interacted with Lap3 during the process, since Atg19 is a cargo receptor for the Cvt pathway. To address this speculation, I performed the following experiments. Firstly, I tested whether Lap3 bound Atg19 using yeast two-hybrid systems as described in "Materials and Methods"; the Lap3-Atg19 interaction, however, was not detected (Figure 30). I next examined the interaction between Atg19 and Lap3 in cell lysates by co-immunoprecipitation analysis. For the experiment, I used *pep4Δatg7Δ* cells both expressing GFP–Lap3 and Atg19–FLAG. Spheroplasts were lysed in the presence of detergent and the lysates were subjected to immunoprecipitation with antibodies against GFP or FLAG. Atg19–FLAG and GFP–Lap3 were co-immunoprecipitated (Figure 31*A*; Figure 31*B*), indicating that Atg19 associates with Lap3 *in vivo*; therefore, Atg19 may be utilized as a receptor for Lap3 transport into the vacuole as Ape1. Besides Ape1 and Ams1, Lap3 is a selective transported protein from cytoplasm to the vacuole, and Lap3 is a novel cargo of the Cvt pathway.

II-B-7 *Lap3 Is Transported to the Vacuole via the Cvt Pathway*

GFP–Ape1 accumulated a dot structure (*e.g.*, the Cvt complex) in *atg7Δ* cells and GFP signal enhanced compared with that of wild-type cells during YPGly growth (data not shown). Correspondingly, endogenously expressing GFP–Lap3 accumulated at the punctate dot and GFP signal increased in *atg7Δ* cells (Figure 32), suggesting the possibility that GFP–Lap3 is recruited

to the Cvt complex during YPGly growth similar to Ape1. GFP–Lap3 also accumulated at a punctate structure in *atg11Δ* and *atg19Δ* cells, and the dot signal of GFP–Lap3 enhanced (Figure 32), indicating that Lap3 is transported to the vacuole via the Cvt pathway. These results are consistent with that of the v-GFP monitoring assay (Figure 28, *lanes 4* and *6*).

II-B-8   *Lap3 Co-localizes with Ape1 at the Extra- and Intravacuolar Dot*

The two classical cargos (Ape1 and Ams1) are engulfed together into the Cvt vesicle and are transported to the vacuole (Figure 5; Figure 6). I examined whether Lap3 was transported to the vacuole together with the classical cargos. GFP–Lap3 co-localized with RFP–Ape1 near the vacuole during YPGly growth in *atg7Δ* cells (Figure 33*A*). Careful observation showed that the GFP–Lap3 and mRFP–Ape1 dots did not merge but were very close to each other. During YPD growth, GFP–Lap3 did not co-localize with RFP–Ape1 (data not shown). I next ascertained whether Lap3 and Ape1 were enwrapped in the Cvt vesicles. GFP–Lap3 was observed the co-localization with RFP–Ape1 inside the vacuole in *pep4Δ* cells, suggesting that it is possible that Lap3 and Ape1 are enwrapped into the same vesicle (Figure 33*B*).

II-B-9   *Lap3 Differs from the Classical Cargo in the Transport Mechanism*

Ape1 homododecameric complex is formed independent of Atg19, whereas Ape1 complex are recruited to the Cvt complex dependent on Atg19 in YPD grown cells. I examined whether accumulation of GFP–Lap3 at the punctate dot requires the Ape1 complex. GFP–Lap3 formed a punctuate dot in the *ape1Δ* and *atg19Δ* cells (Figure 31), and mRFP–Ape1 also formed a punctuate dot in the *lap3Δ* cells (data not shown), indicating that Ape1 complex or Atg19 is not essential for the accumulation of GFP–Lap3 at the punctate structure.

In *ape1Δ* cells, the vacuolar transport of Ams1 was inhibited during YPD growth. In the process of the Cvt pathway, the Ape1 complex is essential for the enwrapment of Ams1 in Cvt vesicles. I investigated whether the Ape1 complex was required for the vacuolar transport of Lap3 during YPGly growth. The cleavage of GFP–Lap3 yielded v-GFP in *ape1Δ* cells at the same level with wild-type cells (Figure 29, *lane 5*), suggesting that Ape1 complex is not essential for the Lap3 transport in contrast to Ams1.

II-B-10   *Lap3 Is an Unstable Protein inside the Vacuole*

The Cvt pathway is contributed to a biosynthetic process for the vacuolar-resident enzymes. Besides Lap3 was selectively transported to the vacuole via the machinery of the Cvt pathway during YPGly growth (Figure 28; Figure 31), Lap3 is a target of selective autophagy under nitrogen-starvation conditions (*Chapter I*). I investigated whether Lap3 also was degraded in the

vacuole during YPGly growth. To analyze a kinetics of Lap3 degradation in the vacuole, I took advantage of a temperature-sensitive *atg1* mutant (*atg1*[ts]) (Shintani and Klionsky, 2004; Suzuki et al., 2001). The *atg1*[ts] cells were grown to mid-log phase ($A_{600} = 0.4$-0.5) at permissive temperature (23°C) and then shifted to non-permissive temperature (37°C) to block Lap3 transport to the vacuole. Samples were taken at the indicated times and followed by immunoblot with anti-Lap3 and anti-Ape1 antisera (Figure 34*A*). At the non-permissive temperature, prApe1 accumulated gradually because of a block in the Cvt pathway, and the amount of mApe1 was maintained within 120 min during the time course (Figure 34*A*, *lanes 3-9*; Figure 34*B*, *closed circle*). GFP–Lap3 also accumulated at the non-permissive temperature, but the amount of v-Lap3 decreased gradually to 50% of its initial level within 90 min and was further degraded (Figure 34*B*, *open circle*).

I also examined whether there remained Lap3 in wild-type and *pep4Δ* cells, respectively. If Lap3 is stable in the vacuole, Lap3 will be detected in the vacuole fraction in wild-type and *pep4Δ* cells. If Lap3 is degraded in the vacuole, Lap3 will be not detected in vacuoles fraction of wild-type cells. Vacuoles were isolated from wild-type and *pep4Δ* cells during YPGly growth and subjected to immunoblot. Prc1 was enriched in the each vacuole fraction, whereas other organelles and the cytoplasm were excluded (Figure 35, *lanes 3* and *4*). Lap3 was maintained in vacuole fraction of *pep4Δ* cells (Figure 35, *lane 4*), whereas Lap3 was not observed in that of wild-type cells (Figure 35, *lane 3*), indicating that Lap3 is degraded in the vacuole dependent on vacuolar hydrolases. The Cvt pathway has ever been defined as the route for vacuole-resident enzymes, which are stable inside the vacuole. Here, I conclude that Lap3 is not a vacuole-resident enzyme but a target to be degraded in the vacuole, and the Cvt pathway plays a crucial role in protein degradation during YPGly growth.

II-C   Discussion

I analyzed the vacuole during YPGly growth and found by proteomic analysis that Lap3 localized at the vacuole (Figure 22*B*). I examined whether Lap3 was transported actually to the vacuole during YPGly growth and observed the behavior of Lap3 using endogenously expressed GFP–Lap3. Then, GFP–Lap3 forms a dot structure and attaches to the Cvt complex (Figure 33*A*). *ATG11* and *ATG19* are essential for Lap3 transport (Figure 28), indicating that Lap3 is selectively transported to the vacuole utilizing similar mechanism to Ape1 under YPGly growth conditions. In *Chapter I*, I demonstrated that Lap3 was degraded in the vacuole during nitrogen starvation. Similarly, GFP-Lap3 is degraded in the vacuole during YPGly growth (Figure 34; Figure 35). Taken together, Lap3 is transported to the vacuole during vegetative growth via Ape1 transport

pathway (the Cvt pathway) and is degraded in the vacuole. The Cvt pathway has traditionally been described as a biosynthetic route, and Atg11 and Atg19 has been believed to be not involved in protein degradation. In this chapter, I propose that machinery of the Cvt pathway also acts for degradation during vegetative growth on non-fermentable medium.

Interestingly, an endogenously expressed GFP–Lap3 is localized in mitochondria and cytoplasm (Figure 25). In addition, GFP–Lap3 is observed as a punctate dot next to the vacuole during YPGly growth, indicating that localization of Lap3 is altered depending on the extracellular environments. To date, the mitochondria-pattern of Lap3, however, has never been visualized distinctly. Previously, the cDNA analysis revealed the presence of in-frame AUG codon upstream of the annotated ORF in the transcripts of Lap3 gene. *LAP3* cDNA is capable of encoding an isoform with a 29-amino acids N-terminal extension, which is mitochondria targeting signal (Miura et al., 2006). Little is known, however, a transcriptional mechanism of it. *LAP3* may use these two transcription start sites to generate mitochondrial and cytoplasmic isoforms reacting to extracellular environments.

GENERAL DISCUSSIONS

I clearly showed that Lap3 is selectively transported to the vacuole via the Cvt complex during vegetative growth and during nitrogen starvation. Lap3 is degraded inside the vacuole, whereas Ape1 retained stably in the vacuole. It is interesting that the fates of Lap3 and Ape1 are different, although the mechanisms of their vacuolar transport are similar. I presents that some cytosolic proteins can be selectively eliminated when they are targeted to the Cvt complex.

1. *Selective Transport of Lap3 into the Vacuole*

I analyzed the behavior of Lap3 during nitrogen starvation using GFP-fused Lap3. In *Chapter I*, the overexpressed GFP–Lap3 (hereafter referred to as GFP–Lap3$^{o/e}$) is not delivered to the vacuole during YPD growth, but is during nitrogen starvation even though it was expressed at a similar level as during nitrogen starvation (Figure 9), indicating that GFP–Lap3 is a target of autophagy but not the Cvt pathway. The time course of GFP–Lap3$^{o/e}$ transport is more rapid than that of a cytosolic protein transport, for example, Ald6 (Figure 11*A*). *ATG11* and *ATG19* are important for Lap3 transport just like Ape1 transport, suggesting that Lap3 is selectively transported to the vacuole by a similar mechanism.

In *Chapter II*, GFP–Lap3 transport was not detectable in cells expressing Lap3 from the endogenous promoter (hereafter simply referred to as GFP–Lap3) even under starvation conditions, probably because expression levels were too low. I next analyzed the behavior of GFP–Lap3 during YPGly growth. Under the conditions, the level of Lap3 is enhanced approximately 15 times as compared with that of YPD grown cells (Figure 24). Furthermore, GFP–Lap3 forms a dot structure and attaches to the Cvt complex (Figure 33*A*). *ATG11* and *ATG19* are essential for Lap3 transport similar to Ape1 (Figure 28). Atg19 is also immunoprecipitated with Lap3, indicating that Atg19 is a receptor for Lap3 transport (Figure 31). Therefore, Lap3 is selectively transported to the vacuole under YPGly growth conditions.

2. *Molecular Mechanisms of Lap3 Sequestration*

Atg17, Atg29, and Atg31 play roles in autophagosome formation as a ternary complex called the Atg17 complex (Kawamata et al., 2008); defects in this complex show little effect on Ape1 transport (Kabeya et al., 2007). Interestingly, in GFP–Lap3$^{o/e}$ overexpressing cells analyzes during nitrogen starvation, Ape1 transport is blocked in *atg29Δ* and *atg31Δ* cells (Figure 14, *lanes 8 and 9*), whereas it seems slightly defective in *atg17Δ* cells (Figure 14, *lane 7*). Similarly, the transport

of GFP–Lap3 is more defective in *atg29Δ* and *atg31Δ* cells than in *atg17Δ* cells (Figure 14, *lanes 2, 7, 8,* and *9*). One possible explanation is that Atg11, a scaffold protein for the Cvt pathway, might be able to behave as an alternative to Atg17, a scaffold protein for autophagosome formation, only in the *atg17Δ* cells during nitrogen starvation.

3. *Accumulation at a Punctate Dot next to the Vacuole*

GFP–Lap3$^{o/e}$ forms a dot co-localizing with Ape1. Interestingly, Lap3 and Ape1 do not form a composite dot, but rather forms distinct dots localized very close to each other (Figure 13). Lap3 is transported to the vacuole even in the absence of Ape1, and the converse is also true, indicating that transports may be independent. Formation of the Ape1 complex depends on its propeptide, as several propeptide mutants defective in Ape1 complex formation are known (Oda et al., 1996; Suzuki et al., 2002). In contrast, Lap3 does not have an apparent propeptide (Johnston, 2004; Miura et al., 2006). I do not know whether GFP–Lap3$^{o/e}$ dot formation is an intrinsic feature or requires other proteins, such as chaperones; however, dot formation is a possible requisite for selective uptake by autophagosomes. On the other hand, I have identified other proteins that form cytoplasmic dots but are not transported to the vacuole (unpublished data). This indicates that a specific receptor(s) is necessary for this type of selective autophagy. Our study suggests that Atg19 behaves as a specific receptor of Lap3.

The mechanism of Lap3 transport resembles those of Ape1. Both Lap3 (Joshua-Tor et al., 1995) and Ape1 (Noda NN and Inagaki F, unpublished data) also form homooligomeric complexes that are concentrated into dots localized in close proximity (Figure 13; Figure 33). Consequently, these dots are enclosed together in the same autophagosomes/autophagic bodies in a manner dependent on Atg19 and Atg11 (Figure 13*B*; Figure 14).

4. *Rate of Lap3 Degradation in the Vacuole*

After GFP–Lap3$^{o/e}$ enters the vacuole, it is cleaved into v-Lap3 and v-GFP, and both can be recognized by immunoblot (Figure 10; Figure 27; Figure 28). As GFP is relatively resistant to vacuolar hydrolases, it can be used as a marker to estimate whether GFP-fused proteins are transported into the vacuole. In this case, v-GFP accumulated under starvation conditions, reflecting in the transport of GFP–Lap3$^{o/e}$ into the vacuole (Figure 9; Figure 26). Lap3 is also detected in the vacuole (Figure 9; Figure 11*A*); I raise the possibility that Lap3 is a vacuolar resident protein. Taking advantage of a temperature-sensitive autophagy mutant, I assessed the lifetime of Lap3 in the vacuole (Figure 12; Figure 34). These results show that Lap3 degrades rapidly after transported to the vacuole; in contrast, mApe1 is stable in the vacuole. Previous

studies described that Lap3 has little activity at vacuolar pH (Enenkel and Wolf, 1993; Xu and Johnston, 1994). Based on these facts, I conclude that Lap3 is not a vacuolar enzyme, but is transported for degradation; however, I cannot exclude the possibility that Lap3 is a short-lived vacuolar enzyme.

5. *Role of the Cvt Pathway in YPGly Grown Cells*

I showed evidence that machinery of the Cvt pathway was involved in protein degradation (*Chapter I* and *Chapter II*) and that constitutive autophagy occurs during vegetative growth. Although the Cvt pathway is believed to be a constitutive and biosynthetic process, the Cvt pathway would be an alternative process to autophagy during growth condition. Studies of the Cvt pathway has ever been performed under a fermentable condition. Further studies on the Cvt pathway under non-fermentable conditions will be crucial in dissecting the role of constitutive autophagy in yeast.

6. *Perspective on this study –Physiological Role of Lap3 Degradation during YPGly Growth-*

Previously, Lap3 was discovered as a protein by its ability to bind to the DNA-recognition sites of the transcriptional activator Gal4 (Xu and Johnston, 1994) and reported as a negative regulator of galactose metabolism (Zheng et al., 1997). Since they found that the expression of Lap3 was regulated by galactose in an expression pattern similar to that of other *GAL* regulatory proteins, the gene encoding the protein was named *GAL6*.

The yeast galactose metabolism has been used as a model for studying transcriptional activation in eukaryotes. On non-fermentable media (*e.g.*, YPGly), the *GAL* structural genes are inactive but withheld for induction (Lohr et al., 1995), with Gal4 on the upstream-activating-sequences (UASgal), and Gal3 presents to mediate induction if galactose becomes available. These *GAL* structural genes are poised for rapid activation during YPGly growth. This rapid inducibility depends on the presence of the induction mediator Gal3. This poised state might have evolved to allow cells a quick response to galactose availability when growing in poorer carbon sources like glycerol.

I demonstrated that during YPGly growth, the endogenous level of Lap3 is enhanced approximately 15 times as compared with that of YPD grown cells (Figure 24). This result shows that Lap3 is up-regulated, whereas Lap3 is degraded in the vacuole. Why Lap3 is degraded during vegetative growth? Here, I make a hypothesis that Lap3 competitively antagonizes Gal3, which localizes at cytoplasm, during YPGly growth. Gal3 is a positive regulator of galactose metabolism,

and Bhat and Hopper previously reported that overproduction of Gal3 causes galactose-independent activation of Gal4 (Bhat and Hopper, 1992). If Gal3 accumulates in cytoplasm, Gal4 may be activated during YPGly growth. Thus, Lap3 may play a crucial role in galactose metabolism by which Lap3 is degraded together with Gal3 in the vacuole (Figure 36).

REFERENCES

Abeliovich, H., W.A. Dunn, Jr., J. Kim, and D.J. Klionsky. 2000. Dissection of autophagosome biogenesis into distinct nucleation and expansion steps. *J. Cell Biol.* 151:1025-34.

Baba, M., M. Osumi, S.V. Scott, D.J. Klionsky, and Y. Ohsumi. 1997. Two distinct pathways for targeting proteins from the cytoplasm to the vacuole/lysosome. *J. Cell Biol.* 139:1687-95.

Baba, M., K. Takeshige, N. Baba, and Y. Ohsumi. 1994. Ultrastructural analysis of the autophagic process in yeast: detection of autophagosomes and their characterization. *J. Cell Biol.* 124:903-13.

Berti, P.J., and A.C. Storer. 1995. Alignment/phylogeny of the papain superfamily of cysteine proteases. *J. Mol. Biol.* 246:273-83.

Bhat, P.J., and J.E. Hopper. 1992. Overproduction of the *GAL1* or *GAL3* protein causes galactose-independent activation of the *GAL4* protein: evidence for a new model of induction for the yeast *GAL/MEL* regulon. *Mol. Cell Biol.* 12:2701-7.

Bryant, N.J., and T.H. Stevens. 1998. Vacuole biogenesis in *Saccharomyces cerevisiae*: protein transport pathways to the yeast vacuole. *Microbiol. Mol. Biol. Rev.* 62:230-47.

Carlson, T., N. Christian, and J.J. Bonner. 1999. A role for RNA metabolism in inducing the heat shock response. *Gene Expr.* 7:283-91.

Enenkel, C., and D.H. Wolf. 1993. *BLH1* codes for a yeast thiol aminopeptidase, the equivalent of mammalian bleomycin hydrolase. *J. Biol. Chem.* 268:7036-43.

Gancedo, J.M. 1998. Yeast carbon catabolite repression. *Microbiol. Mol. Biol. Rev.* 62:334-61.

Hansen, R.J., R.L. Switzer, H. Hinze, and H. Holzer. 1977. Effects of glucose and nitrogen source on the levels of proteinases, peptidases, and proteinase inhibitors in yeast. *Biochim. Biophys. Acta.* 496:103-14.

Hutchins, M.U., and D.J. Klionsky. 2001. Vacuolar localization of oligomeric alpha-mannosidase requires the cytoplasm to vacuole targeting and autophagy pathway components in *Saccharomyces cerevisiae*. *J. Biol. Chem.* 276:20491-8.

Ichimura, Y., T. Kumanomidou, Y.S. Sou, T. Mizushima, J. Ezaki, T. Ueno, E. Kominami, T. Yamane, K. Tanaka, and M. Komatsu. 2008. Structural basis for sorting mechanism of p62 in selective autophagy. *J. Biol. Chem.* 283:22847-57.

Johnston, L.J.-T.a.S.A. 2004. The Bleomycin Hydrolases. *In* Handbook of Proteolytic Enzymes. N.D.R.a.J.F.W. A.J. Barrett, editor. Elsevier, London. 1197-1201.

Joshua-Tor, L., H.E. Xu, S.A. Johnston, and D.C. Rees. 1995. Crystal structure of a conserved protease that binds DNA: the bleomycin hydrolase, Gal6. *Science.* 269:945-50.

Kabeya, Y., T. Kawamata, K. Suzuki, and Y. Ohsumi. 2007. Cis1/Atg31 is required for autophagosome formation in *Saccharomyces cerevisiae*. *Biochem. Biophys. Res. Commun.* 356:405-10.

Kanki, T., and D.J. Klionsky. 2008. Mitophagy in yeast occurs through a selective mechanism. *J. Biol. Chem.*

Kawamata, T., Y. Kamada, Y. Kabeya, T. Sekito, and Y. Ohsumi. 2008. Organization of the Pre-autophagosomal Structure Responsible for Autophagosome Formation. *Mol. Biol. Cell*. 19:2039-50.

Kim, J., S.V. Scott, M.N. Oda, and D.J. Klionsky. 1997. Transport of a large oligomeric protein by the cytoplasm to vacuole protein targeting pathway. *J. Cell Biol.* 137:609-18.

Klionsky, D.J., R. Cueva, and D.S. Yaver. 1992. Aminopeptidase I of *Saccharomyces cerevisiae* is localized to the vacuole independent of the secretory pathway. *J. Cell Biol.* 119:287-99.

Komatsu, M., S. Waguri, M. Koike, Y.S. Sou, T. Ueno, T. Hara, N. Mizushima, J. Iwata, J. Ezaki, S. Murata, J. Hamazaki, Y. Nishito, S. Iemura, T. Natsume, T. Yanagawa, J. Uwayama, E. Warabi, H. Yoshida, T. Ishii, A. Kobayashi, M. Yamamoto, Z. Yue, Y. Uchiyama, E. Kominami, and K. Tanaka. 2007. Homeostatic levels of p62 control cytoplasmic inclusion body formation in autophagy-deficient mice. *Cell*. 131:1149-63.

Kuhn, K.M., J.L. DeRisi, P.O. Brown, and P. Sarnow. 2001. Global and specific translational regulation in the genomic response of *Saccharomyces cerevisiae* to a rapid transfer from a fermentable to a nonfermentable carbon source. *Mol. Cell Biol*. 21:916-27.

Lohr, D., P. Venkov, and J. Zlatanova. 1995. Transcriptional regulation in the yeast GAL gene family: a complex genetic network. *FASEB J*. 9:777-87.

Miura, F., N. Kawaguchi, J. Sese, A. Toyoda, M. Hattori, S. Morishita, and T. Ito. 2006. A large-scale full-length cDNA analysis to explore the budding yeast transcriptome. *Proc. Natl. Acad. Sci. U S A*. 103:17846-51.

Noda, T., A. Matsuura, Y. Wada, and Y. Ohsumi. 1995. Novel system for monitoring autophagy in the yeast *Saccharomyces cerevisiae*. *Biochem. Biophys. Res. Commun.* 210:126-32.

O'Farrell, P.A., F. Gonzalez, W. Zheng, S.A. Johnston, and L. Joshua-Tor. 1999. Crystal structure of human bleomycin hydrolase, a self-compartmentalizing cysteine protease. *Structure*. 7:619-27.

Obara, K., T. Sekito, K. Niimi, and Y. Ohsumi. 2008. The Atg18-Atg2 complex is recruited to autophagic membranes via phosphatidylinositol 3-phosphate and exerts an essential function. *J. Biol. Chem.* 283:23972-80.

Oda, M.N., S.V. Scott, A. Hefner-Gravink, A.D. Caffarelli, and D.J. Klionsky. 1996. Identification of a cytoplasm to vacuole targeting determinant in aminopeptidase I. *J. Cell Biol.* 132:999-1010.

Onodera, J., and Y. Ohsumi. 2004. Ald6p is a preferred target for autophagy in yeast, *Saccharomyces cerevisiae*. *J. Biol. Chem.* 279:16071-6.

Pankiv, S., T.H. Clausen, T. Lamark, A. Brech, J.A. Bruun, H. Outzen, A. Overvatn, G. Bjorkoy, and T. Johansen. 2007. p62/SQSTM1 binds directly to Atg8/LC3 to facilitate degradation of ubiquitinated protein aggregates by autophagy. *J. Biol. Chem.* 282:24131-45.

Piper, R.C., A.A. Cooper, H. Yang, and T.H. Stevens. 1995. *VPS27* controls vacuolar and endocytic traffic through a prevacuolar compartment in *Saccharomyces cerevisiae*. *J. Cell Biol.* 131:603-17.

Reggiori, F., M.W. Black, and H.R. Pelham. 2000. Polar transmembrane domains target proteins to the interior of the yeast vacuole. *Mol. Biol. Cell.* 11:3737-49.

Reggiori, F., I. Monastyrska, T. Shintani, and D.J. Klionsky. 2005. The actin cytoskeleton is required for selective types of autophagy, but not nonspecific autophagy, in the yeast *Saccharomyces cerevisiae*. *Mol. Biol. Cell.* 16:5843-56.

Reggiori, F., and H.R. Pelham. 2001. Sorting of proteins into multivesicular bodies: ubiquitin-dependent and -independent targeting. *EMBO J.* 20:5176-86.

Roberts, G.G., and A.P. Hudson. 2006. Transcriptome profiling of *Saccharomyces cerevisiae* during a transition from fermentative to glycerol-based respiratory growth reveals extensive metabolic and structural remodeling. *Mol. Genet. Genomics.* 276:170-86.

Rolland, F., J. Winderickx, and J.M. Thevelein. 2002. Glucose-sensing and -signalling mechanisms in yeast. *FEMS Yeast Res.* 2:183-201.

Rubinsztein, D.C. 2006. The roles of intracellular protein-degradation pathways in neurodegeneration. *Nature.* 443:780-6.

Scott, S.V., J. Guan, M.U. Hutchins, J. Kim, and D.J. Klionsky. 2001. Cvt19 is a receptor for the cytoplasm-to-vacuole targeting pathway. *Mol. Cell.* 7:1131-41.

Scott, S.V., A. Hefner-Gravink, K.A. Morano, T. Noda, Y. Ohsumi, and D.J. Klionsky. 1996. Cytoplasm-to-vacuole targeting and autophagy employ the same machinery to deliver proteins to the yeast vacuole. *Proc. Natl. Acad. Sci. U S A.* 93:12304-8.

Shintani, T., W.P. Huang, P.E. Stromhaug, and D.J. Klionsky. 2002. Mechanism of cargo selection in the cytoplasm to vacuole targeting pathway. *Dev. Cell.* 3:825-37.

Shintani, T., and D.J. Klionsky. 2004. Cargo proteins facilitate the formation of transport vesicles in the cytoplasm to vacuole targeting pathway. *J. Biol. Chem.* 279:29889-94.

Stromhaug, P.E., F. Reggiori, J. Guan, C.W. Wang, and D.J. Klionsky. 2004. Atg21 is a phosphoinositide binding protein required for efficient lipidation and localization of Atg8 during uptake of aminopeptidase I by selective autophagy. *Mol. Biol. Cell*. 15:3553-66.

Suzuki, K., Y. Kamada, and Y. Ohsumi. 2002. Studies of cargo delivery to the vacuole mediated by autophagosomes in *Saccharomyces cerevisiae*. *Dev. Cell*. 3:815-24.

Suzuki, K., T. Kirisako, Y. Kamada, N. Mizushima, T. Noda, and Y. Ohsumi. 2001. The pre-autophagosomal structure organized by concerted functions of APG genes is essential for autophagosome formation. *EMBO J*. 20:5971-81.

Suzuki, K., Y. Kubota, T. Sekito, and Y. Ohsumi. 2007. Hierarchy of Atg proteins in pre-autophagosomal structure organization. *Genes Cells*. 12:209-18.

Suzuki, K., and Y. Ohsumi. 2007. Molecular machinery of autophagosome formation in yeast, *Saccharomyces cerevisiae*. *FEBS Lett*. 581:2156-61.

Trumbly, R.J., and G. Bradley. 1983. Isolation and characterization of aminopeptidase mutants of *Saccharomyces cerevisiae*. *J. Bacteriol*. 156:36-48.

van der Vaart, A., M. Mari, and F. Reggiori. 2008. A picky eater: exploring the mechanisms of selective autophagy in human pathologies. *Traffic*. 9:281-9.

Xu, H.E., and S.A. Johnston. 1994. Yeast bleomycin hydrolase is a DNA-binding cysteine protease. Identification, purification, biochemical characterization. *J. Biol. Chem*. 269:21177-83.

Yorimitsu, T., and D.J. Klionsky. 2005. Atg11 links cargo to the vesicle-forming machinery in the cytoplasm to vacuole targeting pathway. *Mol. Biol. Cell*. 16:1593-605.

Zheng, W., H.E. Xu, and S.A. Johnston. 1997. The cysteine-peptidase bleomycin hydrolase is a member of the galactose regulon in yeast. *J. Biol. Chem*. 272:30350-5.
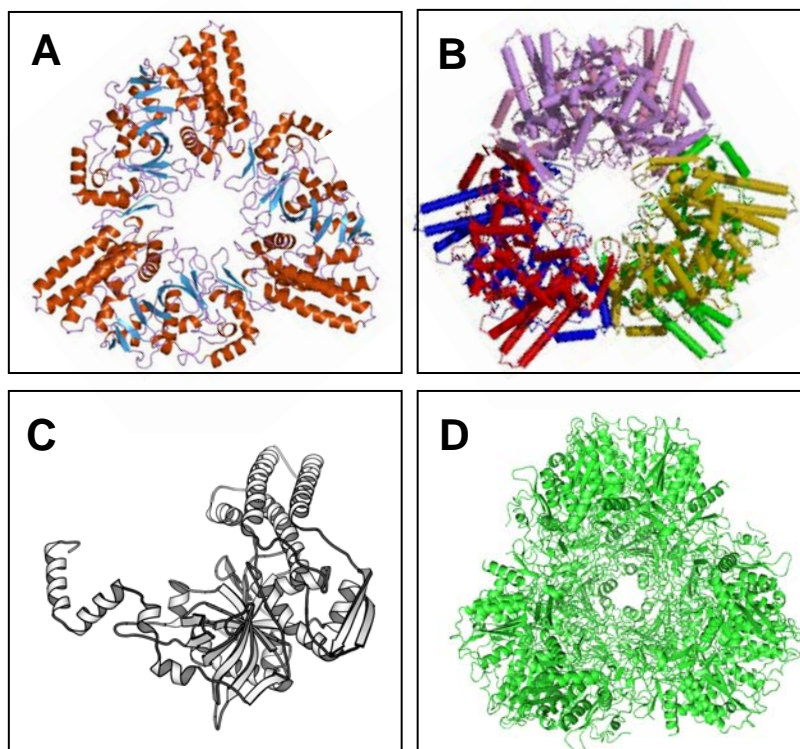
Figure 8. Crystal structures of Lap3 and Lap4/Ape1.

Lap3 is a conserved cysteine protease in both a mammalian and yeast. The central channel is a prominent feature. The structure of the human enzyme is very similar; the three-dimensional structure of the Lap3 hexamer, yeast (*panel A*), mammalian (*panel B*), and subunit structure of Lap3 in yeast (*panel C*). Lap4/Ape1 forms a homododecamer of approximately 750 kDa (*panel D*) (unpublished data; Noda NN and Inagaki F).

	DIC	GFP-Lap3
pep4Δ		
pep4Δ atg7Δ		
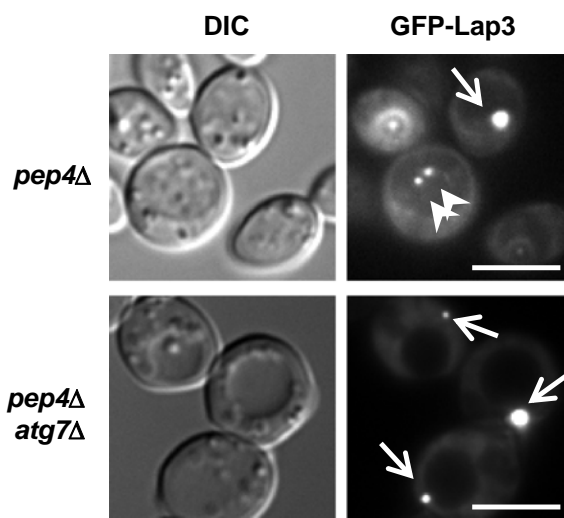
Figure 9. Visualization of Lap3 transport to the vacuole during nitrogen starvation.

The N-terminal GFP tag and the *GPD* promoter were integrated into the genome by homologous recombination. Cells expressing GFP-Lap3 from the *GPD* promoter in the *pep4Δ* (TKY71) or the *pep4Δatg7Δ* (TKY72) background were grown in YPD medium and starved in SD-N medium for 3 h and observed by fluorescence microscopy. Arrowheads indicate dots inside the vacuole. Arrows indicate dot structures in the cytoplasm. DIC, differential interference contrast. Bars, 5 μm.
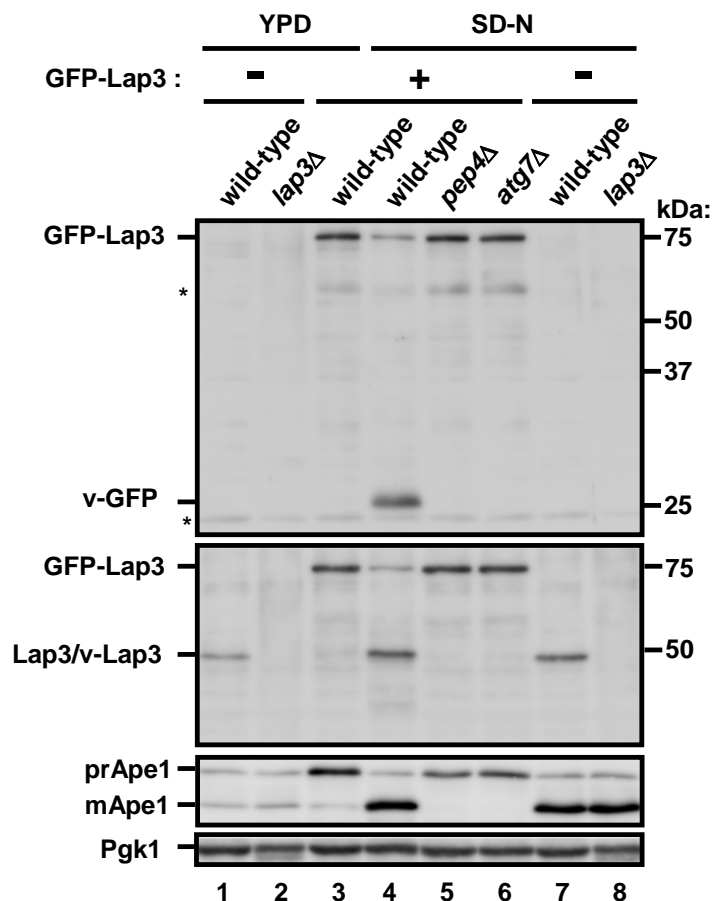
Figure 10. Vacuolar transport of Lap3 during nitrogen starvation.
Cells were grown in YPD medium (*lanes 1-3*) and nitrogen-starved for 5 h (*lanes 4-8*) as described in Figure 9. Cell lysates equivalent to $A_{600} = 0.09$ and $A_{600} = 0.03$ units of cells were subjected to immunoblot analysis with anti-Lap3 and anti-GFP antisera, respectively. Cell lysates equivalent to $A_{600} = 0.2$ and $A_{600} = 0.03$ units of cells were subjected to immunoblot analysis with anti-Ape1 antiserum and anti-Pgk1 antibody. The positions of full length GFP-Lap3, v-GFP, v-Lap3, precursor Ape1 (prApe1), mature Ape1 (mApe1), and Pgk1 are indicated (see the text for details). TKY51 (*lanes 1* and *7*), TKY49 (*lanes 2* and *8*), TKY81 (*lanes 3* and *4*), TKY71 (*lane 5*), and TKY83 (*lane 6*) strains were used. Pgk1 is used as a loading control. The asterisks indicate non-specific bands.

A
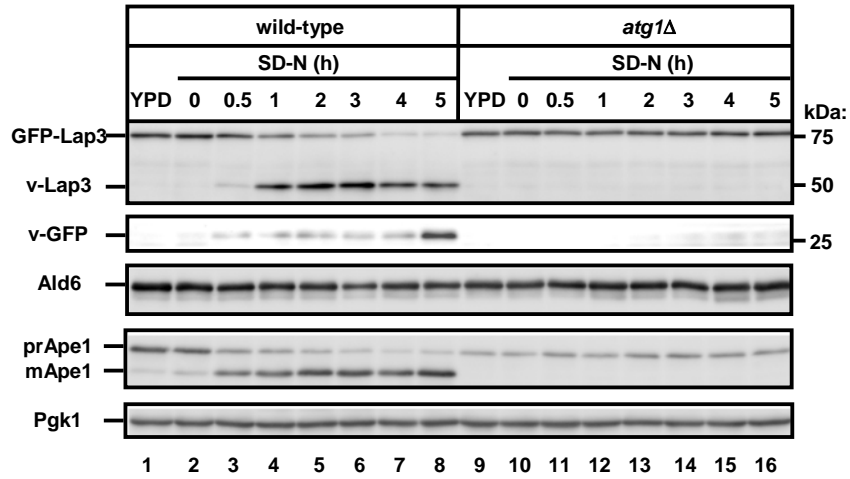
B
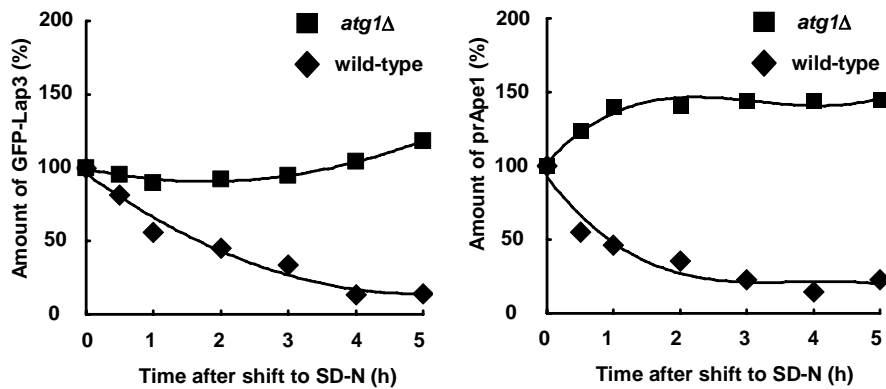
Figure 11. Time course of GFP-Lap3 delivery during starvation.
A, cells were grown to $A_{600} = 1.2$ in YPD medium (*lanes 1* and *9*),
shifted to SD-N medium for 5 h. Cells were collected at the indicated
time points at 0, 0.5, 1, 2, 3, 4, and 5 h (*lanes 2-8* and *10-16*).
Immunoblotting was performed as described in Fig. 9. Wild-type
(TKY81) and *atg1Δ* (TKY82) cells were used. *B,* protein amounts
were estimated using a LAS-4000 system (Fujifilm). The amounts of
GFP-Lap3 and prApe1 were normalized to the amounts of Pgk1
(loading control). The intensity of wild-type (closed square) and
atg1Δ (closed rhombus) cells starved for 0 time in SD-N was set to
100%, respectively.
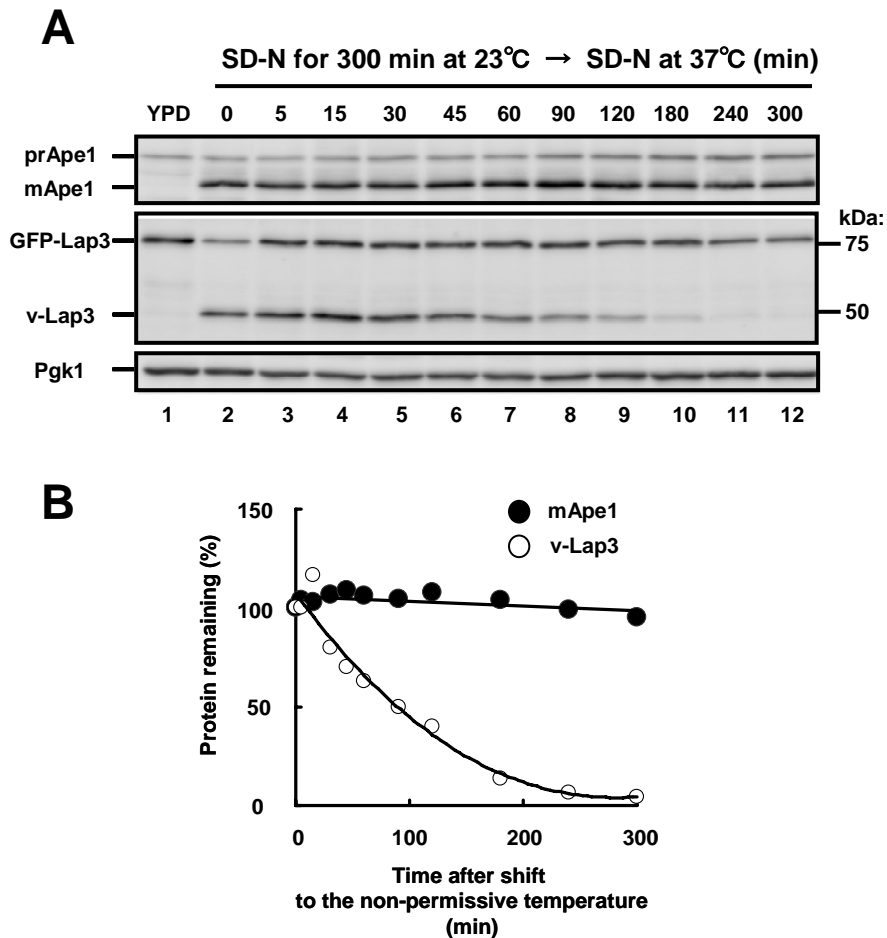
Figure 12. Lap3 degradation in the vacuole using an *atg1* temperature-sensitive-mutant.

A, *atg1ts* cells overexpressing GFP-Lap3 (TKY151) were grown in YPD medium ($A_{600} = 1.2$) at the permissive temperature of $23℃$ (*lane 1*). Cells were shifted to SD-N medium and incubated for 5 h at $23℃$ and were transferred to the non-permissive temperature of $37℃$ and further incubated for 5 h (*lanes 2-12*). Cells were collected at the indicated time points and cell lysates equivalent to $A_{600} = 0.075$ units of cells were subjected to immunoblot analysis with anti-Lap3 antiserum and anti-Pgk1 antibody (loading control). For Ape1, cell lysates equivalent to $A_{600} = 0.15$ units of cells were subjected to immunoblot analysis with an anti-Ape1 antiserum. *B*, protein amounts in Figure 12*A* were estimated as described in Figure 11*B*. The amounts of mApe1 (closed circle) and v-Lap3 (open circle) were normalized to protein amounts at 0 min.
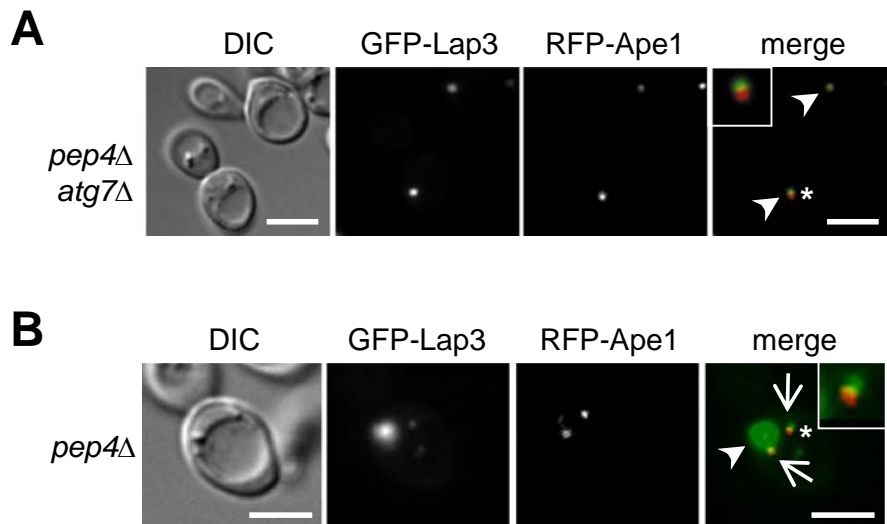
Figure 13. Lap3 localizes to the Cvt complex.

Cells expressing GFP-Lap3 and mRFP-Ape1 were grown in YPD and then incubated in SD-N medium for 3 h. *A*, localization of GFP-Lap3 in *pep4Δatg7Δ* cells (TKY110). *B*, localization of GFP-Lap3 in *pep4Δ* cells (TKY109). The GFP and mRFP signals were observed simultaneously using our microscope system. Arrowheads indicate co-localization of Lap3 and Ape1. Arrows point to intravacuolar structures. Insets are high-magnification images of dots marked with asterisks. GFP-Lap3 and mRFP-Ape1 dots do not merge, but are localized very close to each other. DIC, differential interference contrast. Bars, 5 μm.
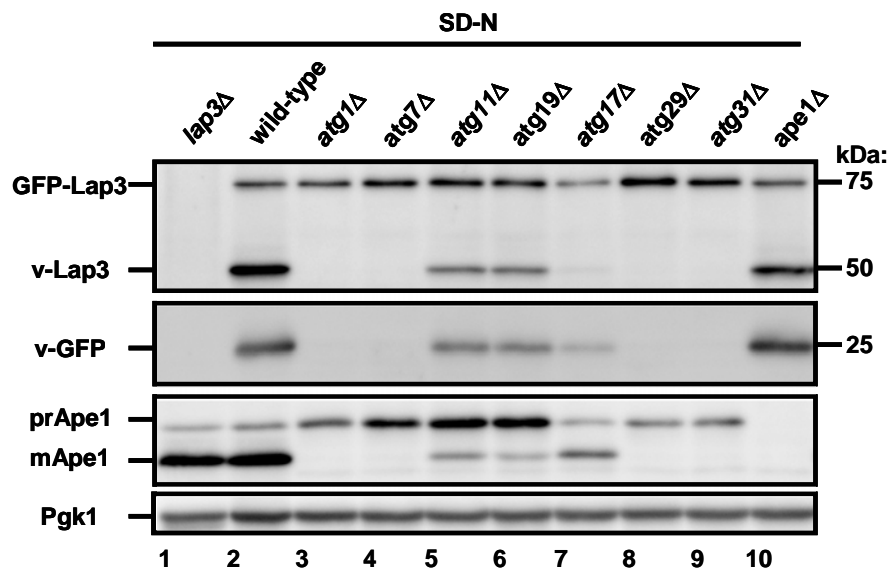
Figure 14. Machinery of the Cvt pathway is involved in Lap3 transport during nitrogen starvation.

GFP-Lap3 transport was monitored by immunoblot for v-Lap3 and v-GFP as described in Figure 10. *lap3Δ* (TKY49), wild-type (TKY81), *atg1Δ* (TKY82), *atg7Δ* (TKY83), *atg11Δ* (TKY84), *atg17Δ* (TKY85), *atg19Δ* (TKY86), *atg29Δ* (TKY89), *atg31Δ* (TKY90), and *ape1Δ* cells (TKY91) were used. Cells starved in SD-N for 5 h.

58
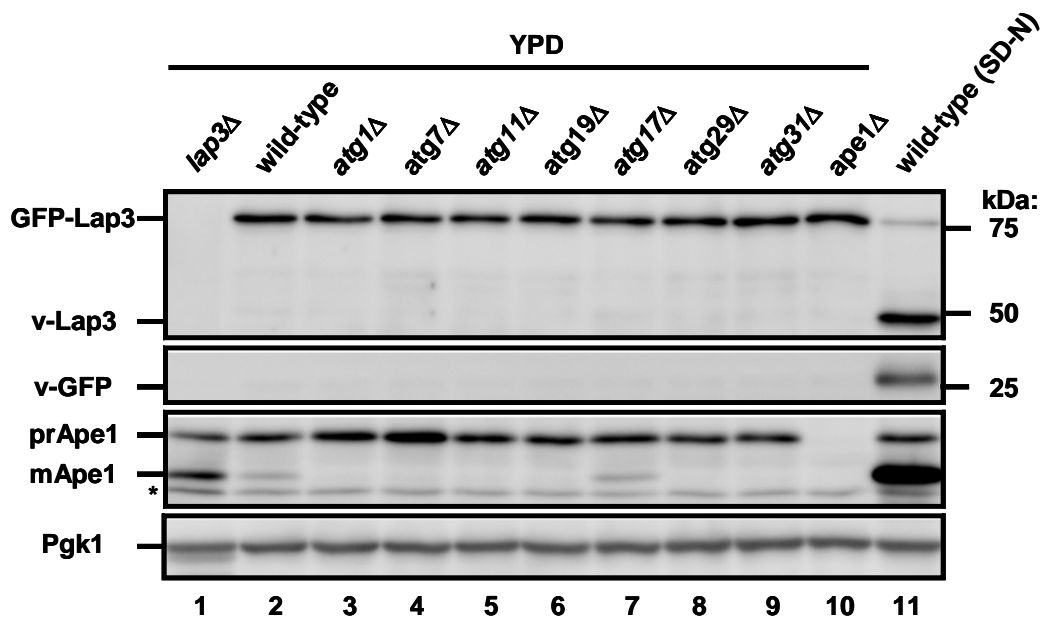
Figure 15. Correlation of the mechanisms for Lap3 transport and Ape1 transport during vegetative growth.

GFP-Lap3 transport was monitored by immunoblot for v-Lap3 and v-GFP as described in Figure 10. *lap3Δ* (TKY49), wild-type (TKY81), *atg1Δ* (TKY82), *atg7Δ* (TKY83), *atg11Δ* (TKY84), *atg17Δ* (TKY85), *atg19Δ* (TKY86), *atg29Δ* (TKY89), *atg31Δ* (TKY90), and *ape1Δ* cells (TKY91) were used. Cells cultured in YPD medium (A_{600} = 1.2) (*lanes 1-10*). The positions of each protein are indicated. The asterisks indicate non-specific bands.
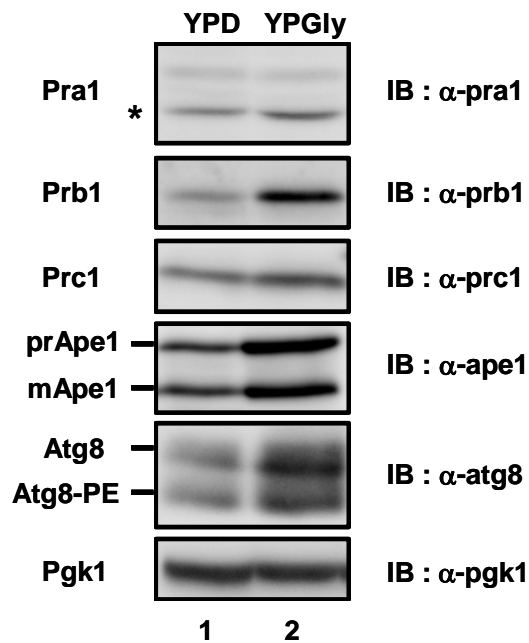
Figure 16. Up-regulation of vacuolar hydrolase during YPGly grown cells.

W303-1A (TKY51) was grown in the YP medium containing Dextrose (YPD, *lane 1*) and glycerol (YPGly, *lane 2*) until a middle logarithmic phase of growth, in respectively. Total cell lysates were prepared as described in material and methods and were subjected to immunoblot with antiserum against indicated markers. The markers are Pra1 (vacuole lumen), Prb1 (vacuole lumen), Prc1 (vacuole lumen), Ape1 (cytosol and vacuole lumen), Atg8 (autophagy- related gene product), and Pgk1 (cytosol). All lanes were loaded with A_{600} = 0.3 units. Star indicated a non-specific band.
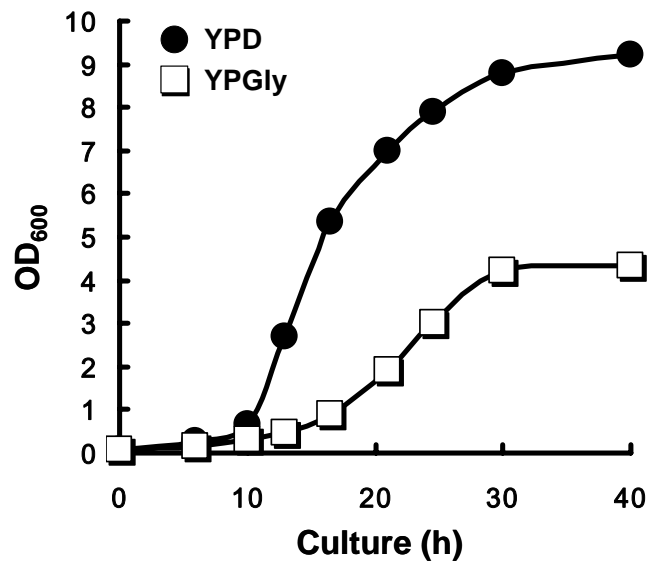
Figure 17. Growth curve of yeast cells in YPD and YPGly media.
   Cells were pre-grown in YPD medium and inoculated at 0.08 OD_{600} cells per ml into YPD (closed circle) and YPGly (open square) and grown at 30℃, respectively, described as "Materials and Methods". This preparation repeats for 40 h. Cells were used wild-type (TKY51). h; hour.

YPD **YPGly**
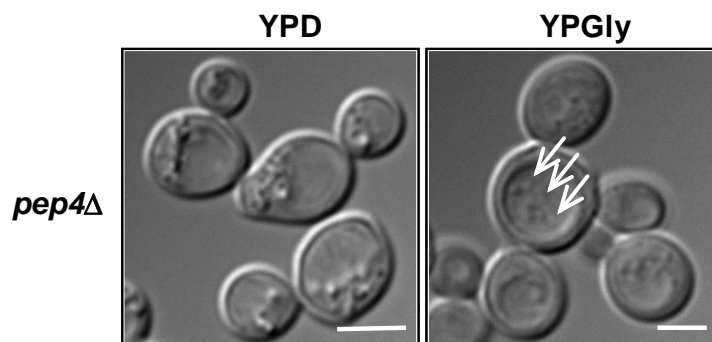
pep4Δ

Figure 18.   Intravacuolar structures accumulate in *pep4*Δ cells during YPGly growth.

　*pep4*Δ cells (TKY46) were grown in YPD medium (*left panel*) and in YPGly medium (*right*) until a middle logarithmic phase of growth, respectively as described in Figure 17 and "Materials and Methods". Cells observed by differential interference contrast (DIC) microscopy. Arrows indicate the intravacuolar structures. Bars, 5 μm.
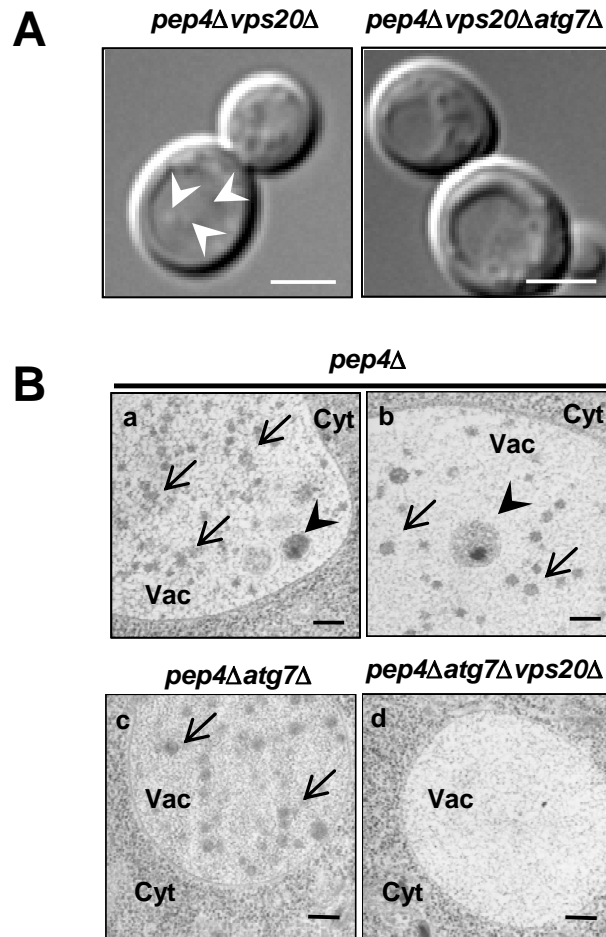
Figure 19. Accumulation of intravacuolar structures is *ATG7*-dependent manner during YPGly growth.

pep4Δ (TKY46; Figure 19*B*, *panel a* and *b*), *pep4Δvps20Δ* (TKY44; Figure 19*A*, *left panel*), and *pep4Δvsp20Δatg7Δ* (TKY45; Figure 19*A*, *right* and Figure 19*B*, *panel d*) were grown in YPG medium as described. *A,* cells observed by DIC microscopy as described. Arrow beads indicate the intravacuolar structures. Bar, 5 μm. *B,* cells observed by electron microscopy. Arrow beads indicate the intravacuolar structures. Arrows indicate multivesicular bodies. Arrowheads indicate the intravacuolar structures dependent on *ATG7*. Cyt, cytoplasm; Vac, vacuole. Bars, 200 nm.
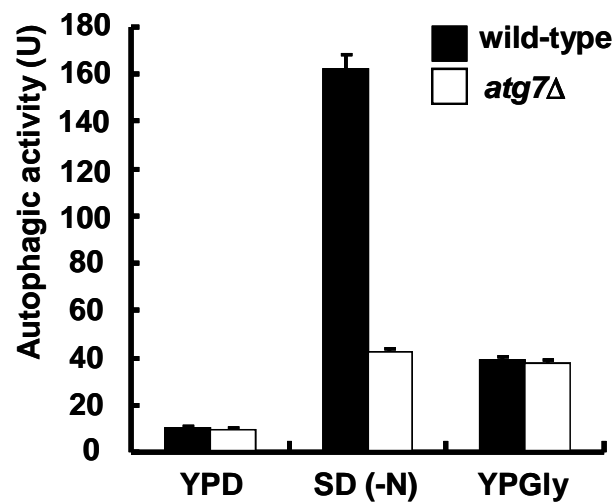
Figure 20.   Non-selective autophagy was undetectable in YPGly grown cells.

Wild-type (TKY52) or *atg7Δ* (TKY53) were cultured in YPD medium to logarithmic phase as described in Figure 17 and then transferred to SD-N for 5 h, lysed and assayed for ALP activity. In YPGly medium, each cells were cultured to logarithmic phase, respectively as descried in Figure 21 (*see below*). After lysed, ALP activity was assayed. The bars represent the standard deviation of three independent experiments.
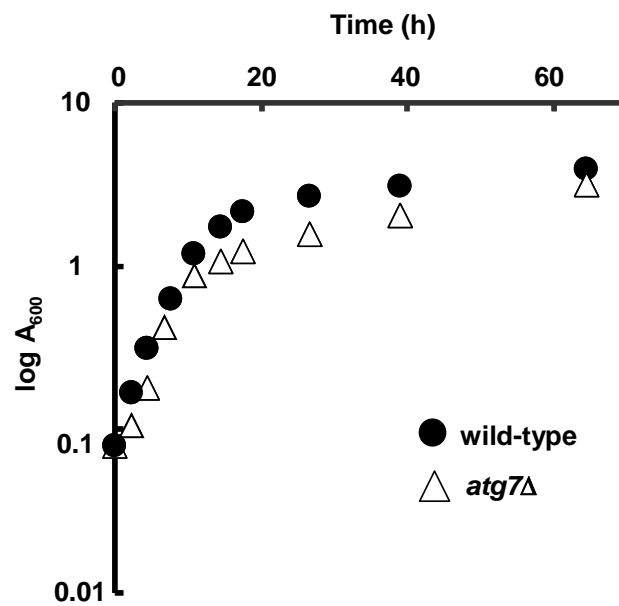
Figure 21. **Growth curve of wild-type and *atg7Δ* cells during YPGly growth.**

Cells were pre-grown in YPD medium and inoculated at 0.08 OD_{600} cells per ml into YPGly medium and grown at 30℃ to logarithmic phase (A_{600} = 0.4-0.5), described as material and method. This preparation repeats for 3 days. Cells were used wild-type (TKY51, closed circle) and *atg7Δ* cells (TYK48, open triangle). h; hour.
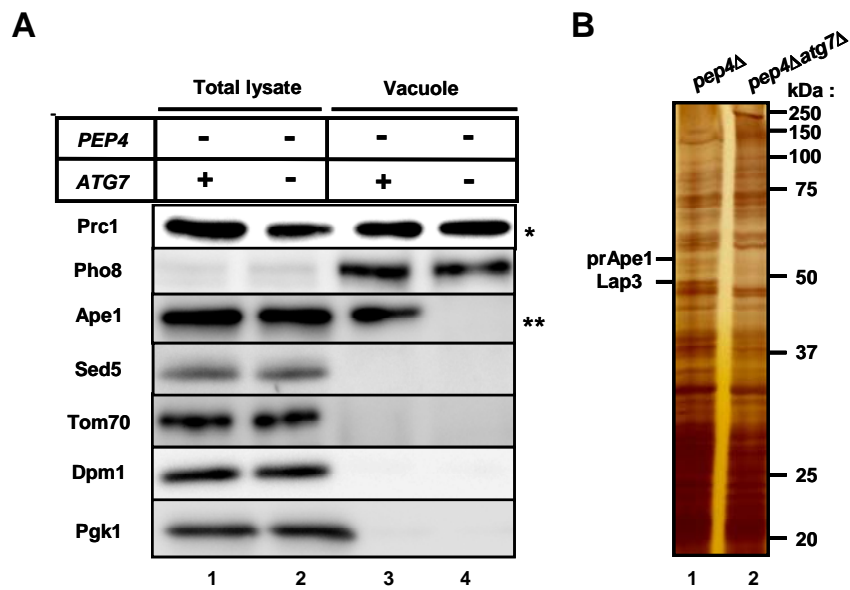
Figure 22. Identification of proteins in the intravacuolar structures.

A, the fractionation procedure was described in the text and "Materials and methods". To confirm purity of the vacuole, immunoblot was used to follow the distribution of proteins in total cell lysates and purified vacuoles. Vacuole markers were used Prc1 and Ape1. Cytosolic marker is Pgk1. Other membrane markers is Sed5 (Golgi), Tom70 (mitochondria), and Dpm1 (ER). *B*, the proteins (25 μg) subjected to SDS-PAGE. After silver stain, MS analysis were performed. Molecular weight markers are indicated on the right (kDa). These were often present in multiple bands, presumably due to proteolysis.
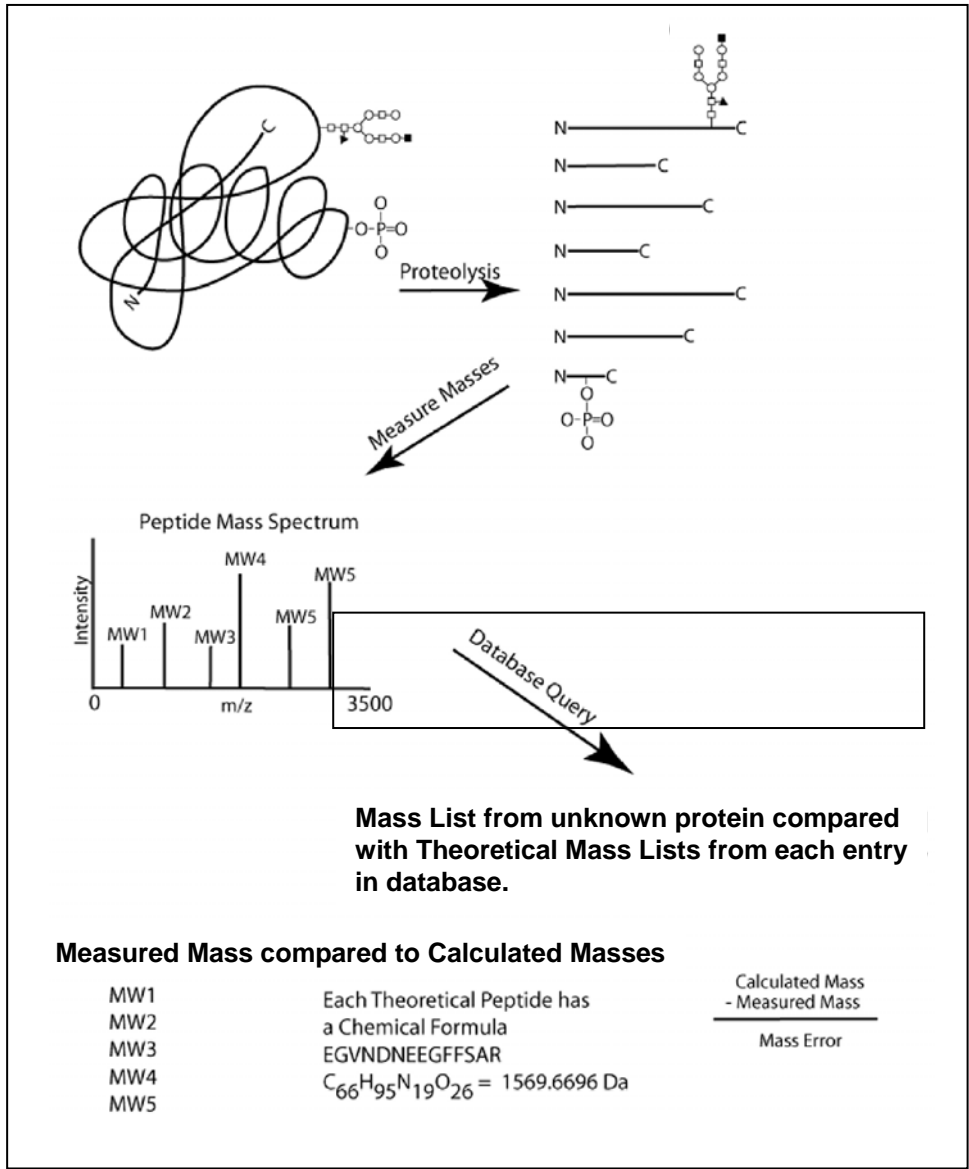
Figure 23.   Illustration of procedures of peptide mass finger-printing (PMF).
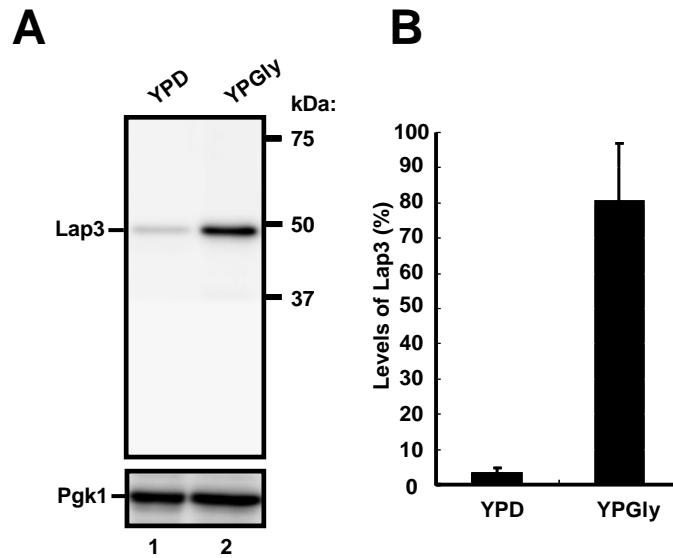
Figure 24.   Quantification of Lap3 in YPD and YPGly growth.
Wild-type cells (TYK51) were cultured in YPD and YPGly medium.   Cells were subjected to immunoblot with antibody against Lap3. *A*, protein amounts were estimated using a LAS-4000 system (Fujifilm). The amount of Lap3 was normalized to the amounts of Pgk1 (loading control). *B*, the intensity of YPD and YPGly was measured, respectively.
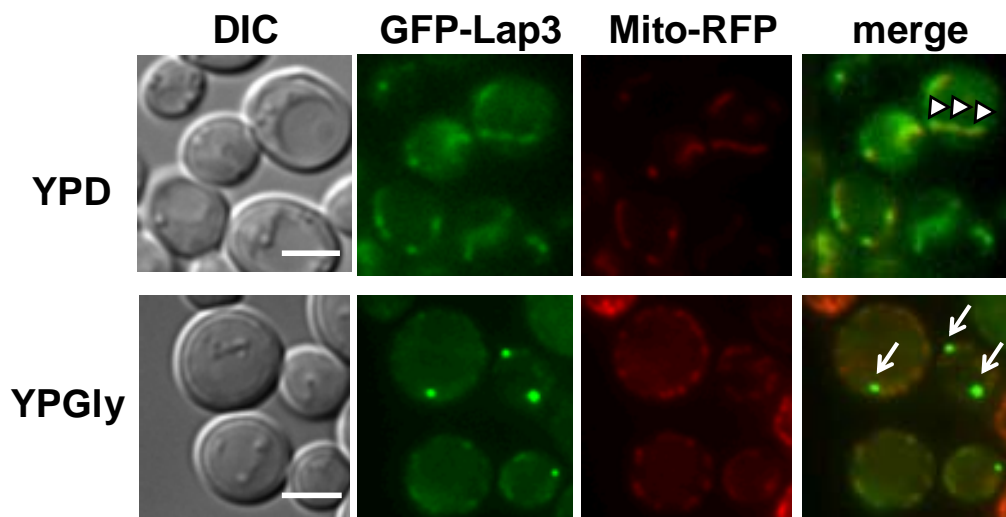
Figure 25. The dynamic alterations of Lap3 localization under growing condition.

Cells integrated GFP-Lap3 using own promoter expression (TKY101) were grown on different carbon sources and observed in logarithmic phase. GFP-Lap3 was located in the cytoplasm and the mitochondria during YPD growth. GFP-Lap3 accumulates at the punctated structure during YPG growth. Cells carrying mito-RFP (TKY107) were grown in YPD and YPGly medium, and observed directly through a GFP, RFP or DIC filter set. Right panells converged image. Arrowheads point to the fluorescent mitochondria signal. Arrows showed a punctated structure near the vacuole. Bars, 4 μm.
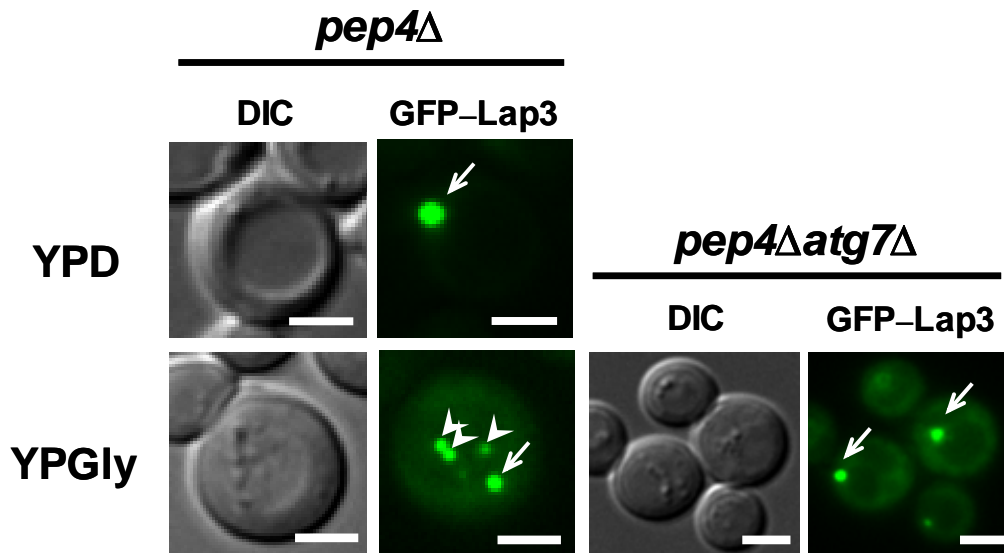
Figure 26. Visualization of Lap3 transport to the vacuole during YPGly growth.

The N-terminal GFP tag and the *GPD* promoter were integrated into the genome by homologous recombination. Cells expressing GFP-Lap3 from the *GPD* promoter in the *pep4Δ* (TKY71) or the *pep4Δatg7Δ* (TKY72) background were grown in YPD and YPGly medium and were observed by fluorescence microscopy. Arrowheads indicate dots inside the vacuole. Arrows indicate dot structures in the cytoplasm. DIC, differential interference contrast. Bars, 5 μm.
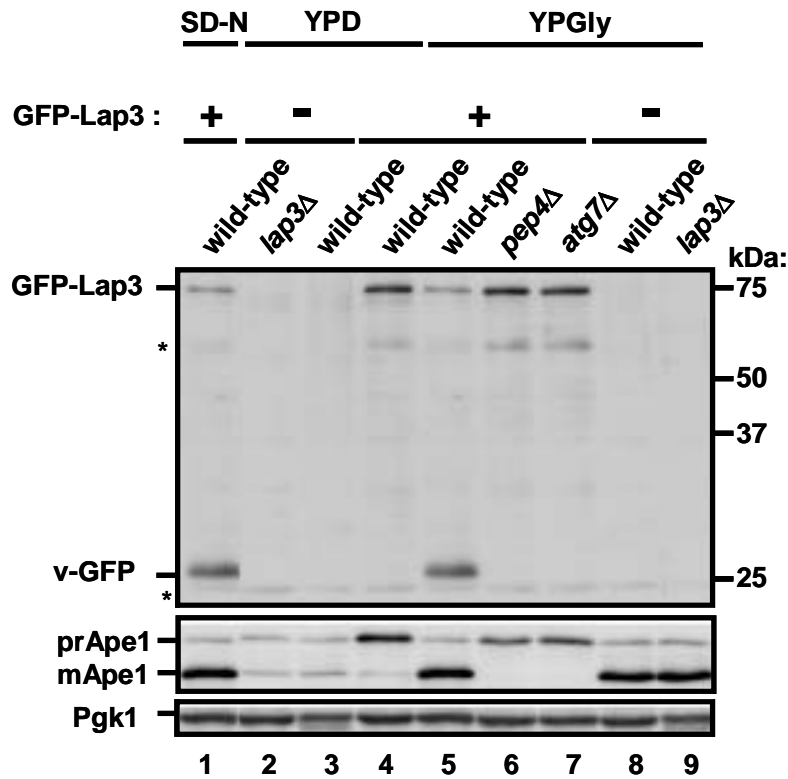
Figure 27. Vacuolar transport of Lap3 during YPGly growth.

Cells were grown in YPD medium (*lanes 2-4*), nitrogen-starved for 5 h (*lane 1*), and YPGly medium (*lanes 5-9*) as described in Figure 24. Cell lysates equivalent to A_{600} = 0.09 and A_{600} = 0.03 units of cells were subjected to immunoblot analysis with anti-GFP antiserum. Cell lysates equivalent to A_{600} = 0.2 and A_{600} = 0.03 units of cells were subjected to immunoblot analysis with anti-Ape1 antiserum and anti-Pgk1 antibody. The positions of full length GFP-Lap3, v-GFP, precursor Ape1 (prApe1), mature Ape1 (mApe1), and Pgk1 are indicated (see the text for details). TKY51 (*lanes 3* and *8*), TKY49 (*lanes 2* and *9*), TKY81 (*lanes 1, 4,* and *5*), TKY71 (*lane 6*), and TKY83 (*lane 7*) strains were used. Pgk1 is used as a loading control. The asterisks indicate non-specific bands.
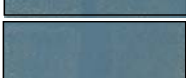
71
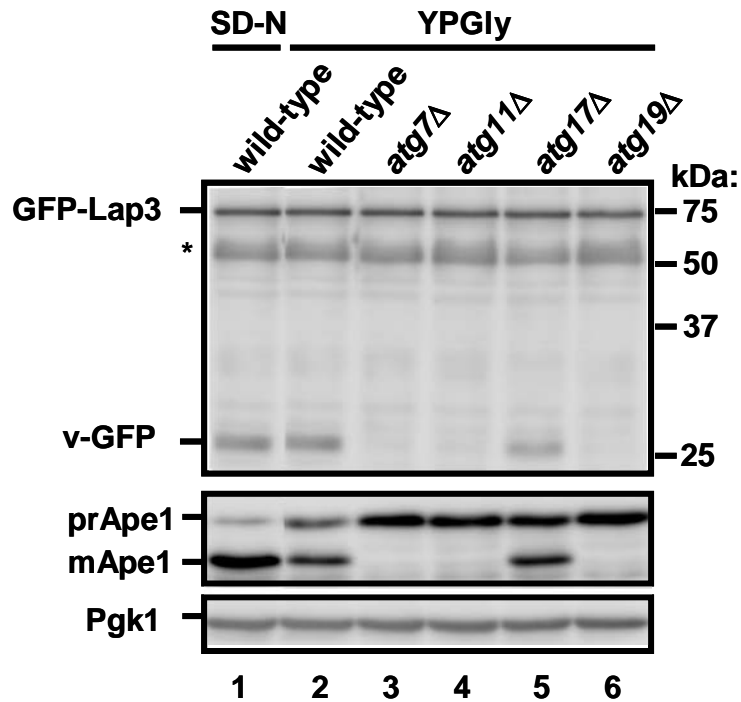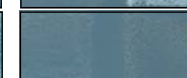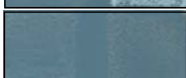
Figure 28.   Requirement of Atg11 and Atg19 for Lap3 transport during YPGly growth.

GFP-Lap3 transport was monitored by immunoblot for v-GFP as described in Figure 24. *lap3Δ* (TKY49), wild-type (TKY81), *atg7Δ* (TKY83), *atg11Δ* (TKY84), *atg17Δ* (TKY85), *atg19Δ* (TKY86) were used. Cells cultured in YPGly medium (A_{600} = 0.4-0.5) (*lanes 1-6*). The positions of each protein are indicated. The asterisk indicates non-specific bands.
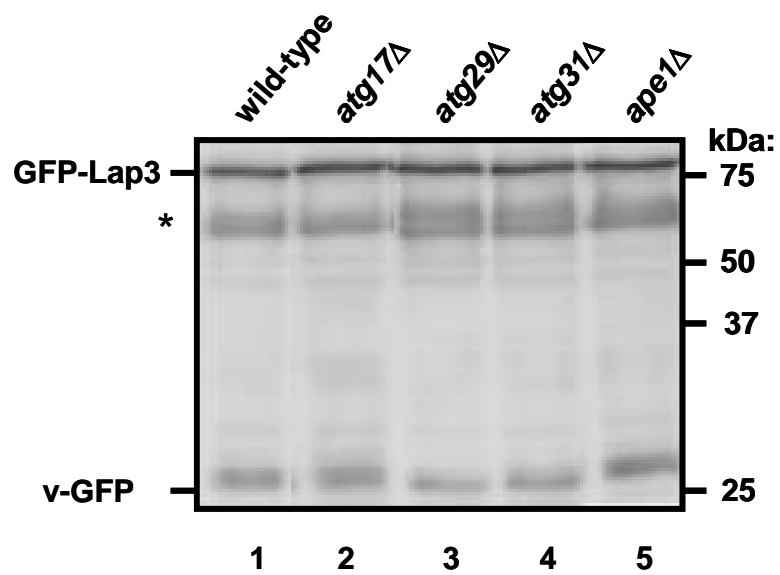
Figure 29. Atg17 complex is not essential for Lap3 transport during YPGly growth.

GFP-Lap3 transport was monitored by immunoblot for v-GFP as described in Figure 24. Wild-type (TKY81), *atg17Δ* (TKY85), *atg29Δ* (TKY89), *atg31Δ* (TKY90), and *ape1Δ* cells (TKY91) were used. Cells cultured in YPGly medium (A_{600} = 0.4-0.5) (*lanes 1-5*). The positions of each protein are indicated. The asterisk indicates non-specific bands.

|	1	2	-LW 1	-LW 2	-ALW 1	-ALW 2
	Lap3 / Lap3	Ape1 / Ape1				
	Atg19 / Lap3	Atg19 / Ape1				
	Lap3 / Atg8	Atg8 / Lap3				
	Lap3 / Atg11	Atg11 / Lap3				
	Lap3 / Ape1	Ape1 / Lap3				

* pGAD- / pGBD-

Figure 30. The Lap3-Atg19 interaction is undetectable in yeast two-hybrid systems.

Cells (PJ69-4A) were transformed with the yeast two-hybrid assay plasmids pGAD and pGBD that encode the indicated proteins or none (empty; data not shown) and grown on SGly -LW and SGly –ALW, respectively for 7 days.
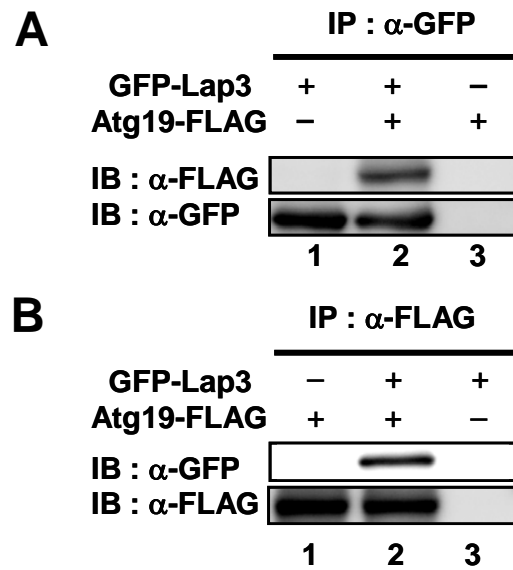
Figure 31. Co-immunoprecipitation of Lap3 and Atg19.

A and *B*, spheroplasts in YPG isolated from *pep4Δatg7Δ* cells containing C-terminally FLAG tagged Atg19 on integration (TKY142), and lysed in native immunoprecipitation buffer. The resulting extract was cleared by centrifugation at *700 xg* for 10 min before immunoprecipitating with antisera as indicated by "First Ab." A second, nonnative immunoprecipitation reaction was then performed using the antisera denoted as "Second Ab." (*see text*). The positions of Atg19-FLAG, and GFP-Lap3 are indicated.
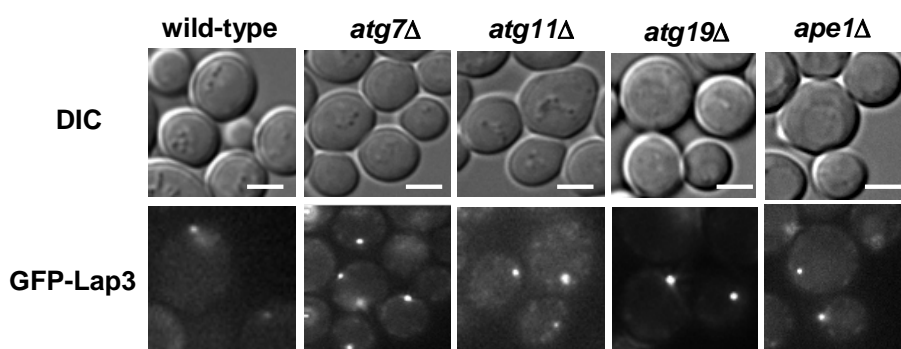
Figure 32. Enhancement of GFP-Lap3 signal at the punctate dot in *atg* mutants.

The wild type (TKY51), *atg7Δ* (TKY102), *atg11Δ* (TKY103), *atg19Δ* (TKY105), and *ape1Δ* (TKY106) cells expressing GFP-Lap3 from its own promoter were grown in YPGly to logarithmic phase. Cells were observed directly through a GFP and DIC filter set. Bars, 4 μm.
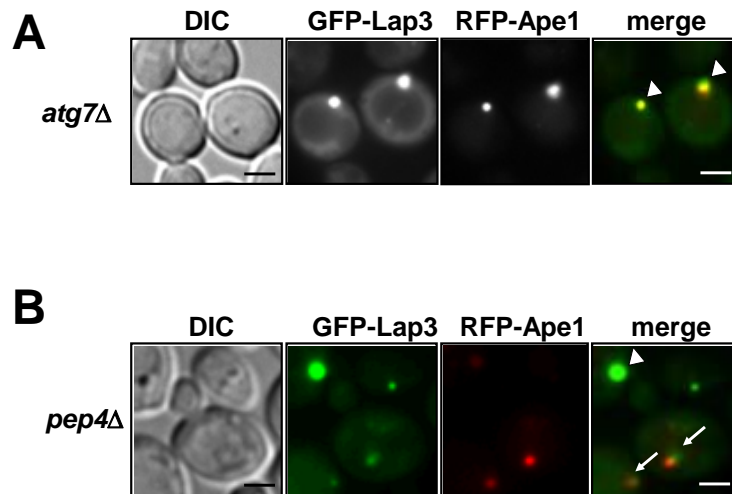
Figure 33. Lap3 localizes to the Cvt complex during YPGly growth.

Cells expressing GFP-Lap3 and mRFP-Ape1 were grown in YPGly medium. *A*, localization of GFP-Lap3 in *atg7Δ* cells (TKY108). *B*, localization of GFP-Lap3 in *pep4Δ* cells (TKY109). The GFP and mRFP signals were observed simultaneously using our microscope system. Arrowheads indicate co-localization of Lap3 and Ape1. Arrows point to intravacuolar structures. GFP-Lap3 and mRFP-Ape1 dots do not merge, but are localized very close to each other. DIC, differential interference contrast. Bars, 4 μm.
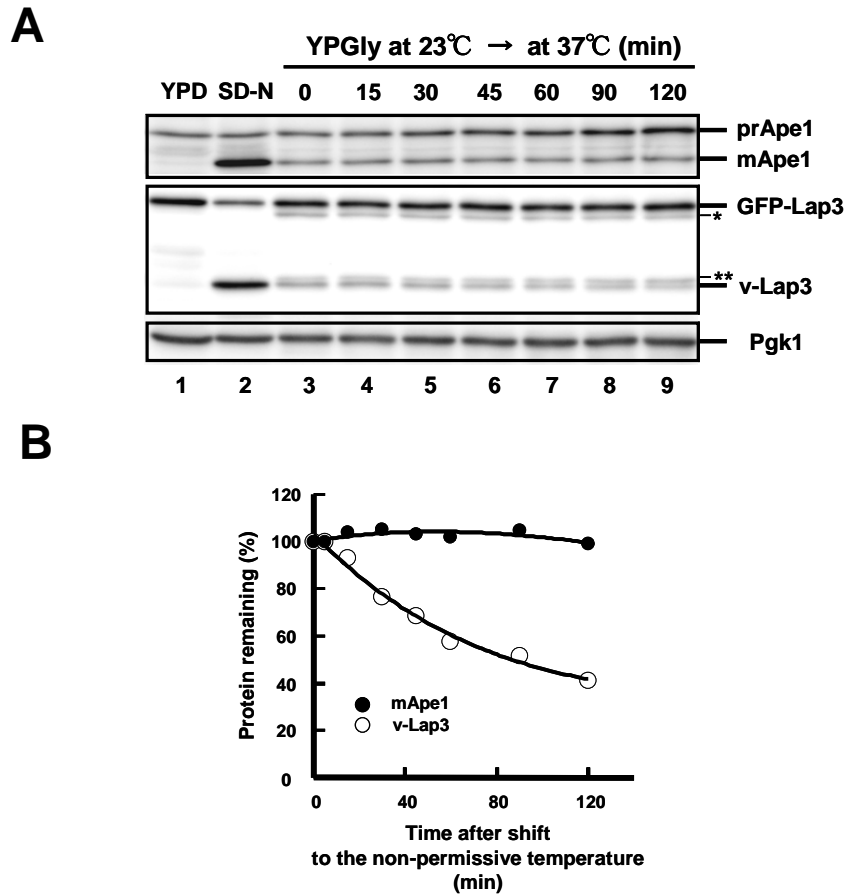
Figure 34. Lap3 degradation in the vacuole using an *atg1* temperature-sensitive mutant during YPGly growth.

A, atg1^{ts} cells overexpressing GFP-Lap3 (TKY151) were grown in YPGly medium (A_{600} = 0.4-0.5) at the permissive temperature of 23°C (*lane 1*). Cells then were transferred to the non-permissive temperature of 37°C (*lanes 3-12*). Cells were collected at the indicated time points and cell lysates (3 μg) were subjected to immunoblot analysis with anti-Lap3 antiserum and anti-Pgk1 antibody (loading control). For Ape1, cell lysates (5 μg) were subjected to immunoblot analysis with an anti-Ape1 antiserum. *B*, protein amounts in Figure 33*A* were estimated as described in Fig. 12*B*. The amounts of mApe1 (closed circle) and v-Lap3 (closed square) were normalized to protein amounts at 0 min.

	Total lysate		Vacuole	
PEP4	+	-	+	-
Lap3				
Prc1				
Tom70				
Dpm1				
Pgk1				
	1	2	3	4

p2
mPrc1
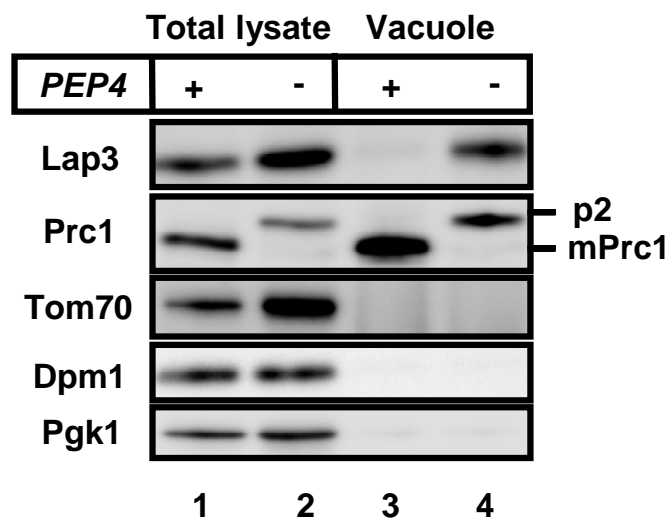
Figure 35. Lap3 is degraded in the vacuole.
Immunoblot analyses of total lysates from intact cells and isolated vacuoles from wild-type (TKY51) and *pep4Δ* (TKY46) cells. The blots were probed with antiserum against Lap3, Prc1, Tom70, and antibodies against Dpm1 and Pgk1. All lanes were loaded with 1 µg protein and subjected to SDS-PAGE as described in "Material and Methods".
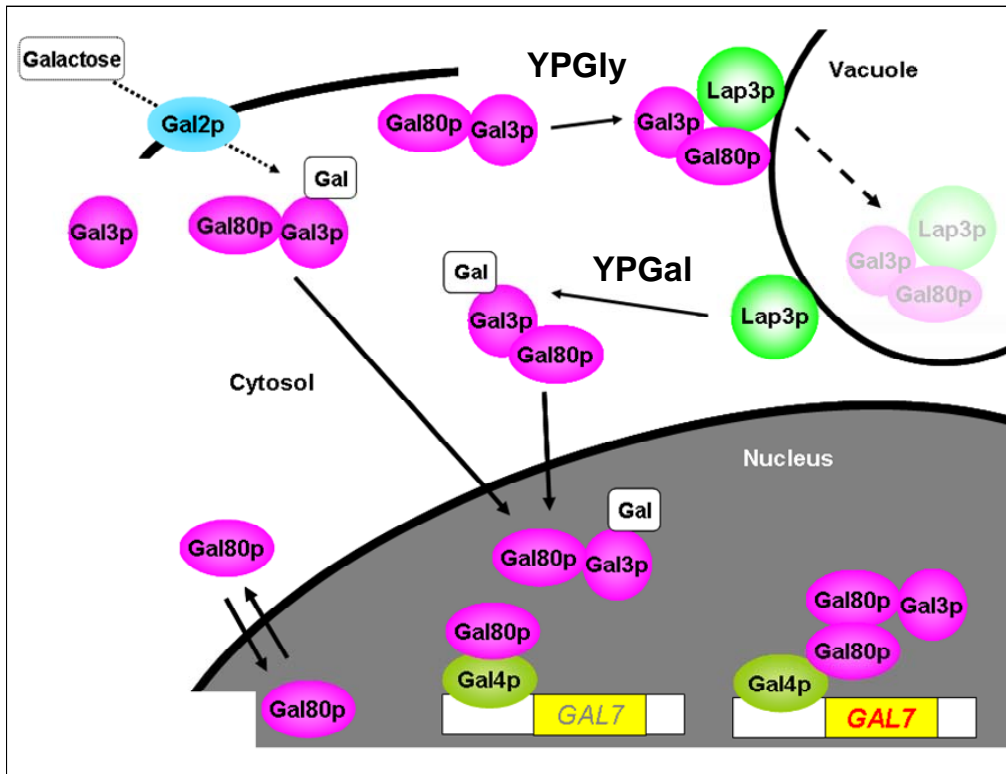
Figure 36. **Model of the *GAL* regulation involved Autophagy under YPGly growth conditions.**